

Discovery of a Candidate Containing an (*S*)-3,3-Difluoro-1-(4-methylpiperazin-1-yl)-2,3-dihydro-1*H*-inden Scaffold as a Highly Potent Pan-Inhibitor of the BCR-ABL Kinase Including the T315I-Resistant Mutant for the Treatment of Chronic Myeloid Leukemia

Dongfeng Zhang,[▽] Peng Li,[▽] Yongxin Gao, Yaoyao Song, Yaqin Zhu, Hong Su, Beibei Yang, Li Li, Gang Li, Ningbo Gong, Yang Lu, Huanjie Shao,* Chunrong Yu,* and Haihong Huang*

Cite This: *J. Med. Chem.* 2021, 64, 7434–7452

Read Online

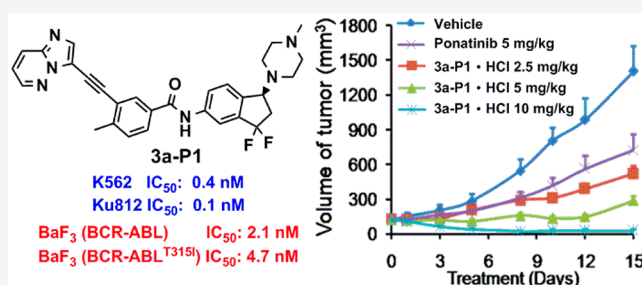
ACCESS |

Metrics & More

Article Recommendations

Supporting Information

ABSTRACT: BCR-ABL kinase inhibition is an effective strategy for the treatment of chronic myeloid leukemia (CML). Herein, we report compound **3a-P1**, bearing a difluoro-indene scaffold, as a novel potent pan-inhibitor against BCR-ABL mutants, including the most refractory T315I mutant. As the privileged (*S*)-isomer compared to its (*R*)-isomer **3a-P2**, **3a-P1** exhibited potent antiproliferative activities against K562 and Ku812 CML cells and BCR-ABL and BCR-ABL^{T315I} BaF3 cells, with IC₅₀ values of 0.4, 0.1, 2.1, and 4.7 nM, respectively. **3a-P1** displayed a good safety profile in a battery of assays, including single-dose toxicity, hERG K⁺, and genotoxicity. It also showed favorable mice pharmacokinetic properties with a good oral bioavailability (32%), a reasonable half-life (4.61 h), and a high exposure (1386 h·ng/mL). Importantly, **3a-P1** demonstrated a higher potency than ponatinib in a mice xenograft model of BaF3 harboring BCR-ABL^{T315I}. Overall, the results indicate that **3a-P1** is a promising drug candidate for the treatment of CML to overcome the imatinib-resistant T315I BCR-ABL mutation.



INTRODUCTION

Chronic myeloid leukemia (CML) results in a malignant tumor and is characterized by the production of a large number of immature white blood cells, which accumulate in the bone marrow and inhibit normal hematopoietic function. Most CML cases are driven by the breakpoint cluster region-abelson leukemia virus (BCR-ABL), which constitutes an activated fusion tyrosine kinase formed by the translocation of the Philadelphia chromosome (Ph) between the ABL oncogene from the long arm of chromosome 9 and the BCR from the long arm of chromosome 22.^{1,2}

Imatinib (Figure 1) is a first-generation BCR-ABL inhibitor and is highly effective in approximately 60% of CML patients.³ However, the acquired resistance to imatinib has become a major challenge for the clinical management of CML.⁴ Significant efforts have been devoted to identifying novel BCR-ABL inhibitors to overcome imatinib resistance. Nilotinib, dasatinib, and bosutinib have been approved as second-generation drugs to treat adult patients in all phases of CML with an acquired resistance to imatinib.^{5–7} However, these second-generation inhibitors do not target the most refractory mutant of BCR-ABL, T315I.⁸

To date, the only approved third-generation inhibitor for CML is ponatinib⁹ (Figure 1), which has been demonstrated

to inhibit native ABL, BCR-ABL, BCR-ABL^{T315I}, and other clinically important ABL kinase domain mutants (i.e., Q252H, Y253H, M351T, and H396P). Additionally, ponatinib also inhibits the sarcoma gene (SRC) and members of the vascular endothelial growth factor receptor (VEGFR), fibroblast growth factor receptor (FGFR), and platelet-derived growth factor receptor (PDGFR) families of receptor tyrosine kinases.¹⁰ Although the Food and Drug Administration (FDA) issued a black-framed warning of the cardiovascular risk and liver toxicity of ponatinib as a multitarget tyrosine kinase inhibitor, ponatinib was recently proven to be a valuable alternative treatment to allogeneic stem cell transplantation in patients with T315I-positive advanced CML and Philadelphia-chromosome-positive (Ph⁺) acute lymphoblastic leukemia.¹¹

Among the more than 100 resistant mutants of BCR-ABL that have been clinically identified, the “gatekeeper” T315I is the most common mutation, accounting for approximately

Received: January 17, 2021

Published: May 20, 2021



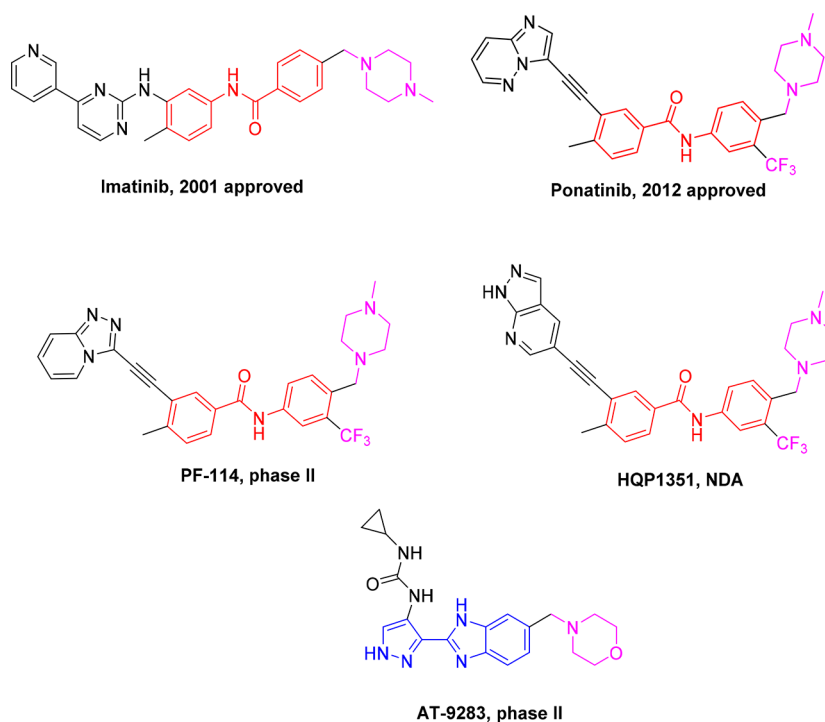


Figure 1. Chemical structures of BCR-ABL inhibitors.

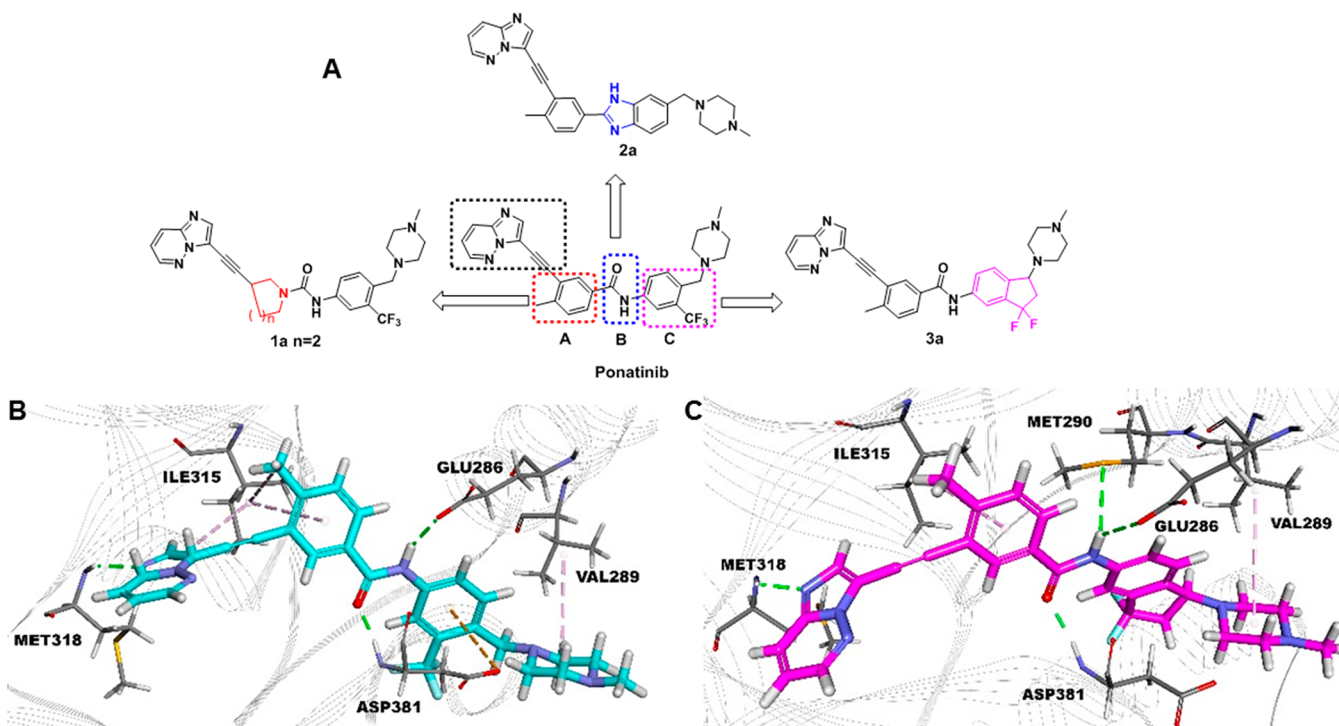


Figure 2. (A) Design strategy for ponatinib-based BCR-ABL kinase inhibitors. (B) Crystal structure of ponatinib in a complex with the BCR-ABL^{T315I} mutant kinase (PDB 3IK3). Ponatinib is shown in cyan. (C) The predicted binding modes of 3a with the BCR-ABL^{T315I} mutant kinase (PDB 3IK3). 3a is shown in pink, hydrogen bonds are shown as green dashed lines, and van der Waals interactions are shown as magenta dashed lines.

15%–20% of all clinically acquired mutants.¹² The T315I mutation stops the binding of ATP-competitive inhibitors to the ABL catalytic domain by either direct steric hindrance or stabilizing the active kinase conformation. The development of new drugs to target the open and active conformation of the T315I mutant is therefore a major challenge. Several small-

molecule inhibitors targeting BCR-ABL^{T315I} have been reported (Figure 1), among which PF-114¹³ and AT-9283^{14,15} are in clinical phase II investigations and exhibit potent inhibitory activities toward the BCR-ABL^{T315I} mutant. HQP1351,¹⁶ developed by Ascentage Pharma, has completed its phase II clinical trial, and a New Drug Application (NDA)

has been submitted to regulators in China. Therefore, the development of structurally distinct BCR-ABL inhibitors, particularly, those capable of inhibiting the mutant T315I, would facilitate drug discovery for CML treatment.

Herein, we report the design and evaluation of **3a-P1** bearing a novel difluoro-indene scaffold with the privileged (S)-configuration, which is a new orally bioavailable pan-BCR-ABL inhibitor with a high potency against T315I and several other BCR-ABL mutants, including p-loop region mutants (G250E, Q252H, Y253F, and E255K), an ATP-binding domain hinge region mutant (F317L), a catalytic segment mutant (M351T), and an activation loop region mutant (H396P). The compound **3a-P1** is more potent than ponatinib in mouse xenograft models of BCR-ABL^{T315I}-driven tumor growth. Furthermore, **3a-P1** exhibits an acceptable safety profile as evaluated by preliminary safety assessments, including hERG channel inhibition assay, the Ames test, chromosome aberration, bone marrow micronucleus, and single-dose toxicity assessments.

RESULTS AND DISCUSSION

It was evident that most of the reported BCR-ABL inhibitors have an amide group between two aryl rings, a heterocycle tail, and an aryl group head. Furthermore, it was established that the arylacetylene (head) and *N*-methylpiperazine (tail) motifs of ponatinib and its analogues are important for their activities against the gatekeeper mutant BCR-ABL^{T315I}.^{9,16} On the basis of this analysis, we intended to exploit structural modifications of the A (left phenyl ring), B (amide group), and C (right phenyl ring) regions of ponatinib to achieve the goal of identifying novel chemical scaffolds with potent activities toward the BCR-ABL^{T315I} mutant and improved drug-like properties (Figure 2A).

As disclosed in Figure 2B, the crystal structure of ponatinib in a complex with the BCR-ABL^{T315I} mutant kinase (PDB 3IK3) revealed that the slim alkyne linker between the diarylamide scaffold and the imidazo[1,2-*b*]pyridazine motif is crucial to the success of ponatinib, as it avoids a steric clash with a bulky isoleucine residue at the gatekeeper position. Additionally, the ethynyl linkage and phenyl group in the A region of ponatinib have favorable van der Waals interactions with the Ile315 mutated residue. Moreover, the *N*-methylpiperazinyl group of ponatinib occupies the pocket formed by the P-loop, the DFG motif, and the catalytic loop and thus plays an important role in the key interactions (Figure 2B). According to the analysis of the crystal structure and our general optimization strategies, we first used a heterocycle to replace the phenyl group of ponatinib in the A region to generate piperidine compound **1a** with a ClogP of 3.62, which was lower than that of ponatinib (ClogP 5.77) (Figure 2A). It is likely that the van der Waals interactions of the heterocycle derivative **1a** with Ile315 were enhanced because of the introduction of piperidine. Inspired by the unique structure of AT-9283, which contains a benzimidazole fragment, we replaced the amide group with an imidazole group, as exemplified by compound **2a** containing the benzimidazole scaffold, through a bioisosterism strategy. Considering the potential cardiovascular risk displayed by ponatinib due to the moderate inhibition of the hERG K⁺ channel, the difluoro-indene moiety was introduced to the C region, therefore keeping the key methylpiperazine group and taking advantage of a cyclization strategy to generate **3a** with the aim of reducing

the hERG inhibition by enhancing the confirmation rigidity and lowering the lipophilicity (ClogP 4.69) of **3a**.

Subsequently, we selected compound **3a** for a computational study to investigate its potential binding mode with BCR-ABL^{T315I}. The study predicted that the nitrogen atom in the imidazo[1,2-*b*]pyridazine group of **3a** would form a hydrogen bond with the aminocarbonyl oxygen of Met318 in the ABL kinase. A gatekeeper isoleucine residue was found at the interface formed by the van der Waals contacts between compound **3a** and the T315I mutant of ABL (Figure 2C), which indicated that favorable hydrophobic interactions were occurred with the T315I mutant. Interestingly, the hydrogen in the amide group of **3a** formed a hydrogen bond with Met290, which was different from the interactions of ponatinib and indicated that compound **3a** may have better potency than ponatinib.

The *in vitro* potencies of the designed compounds **1a**, **1b**, **2a–2k**, and **3a–3e** were first assessed against K562, a CML cell line harboring native BCR-ABL, with ponatinib included for comparison. As shown in Table 1, compounds **1a** and **1b** showed activities similar to that of ponatinib. The compounds with a benzimidazole core (**2a–2k**), where R₁ is either imidazo[1,2-*b*]pyridazine (**2a** and **2g**) or *N*-cyclopropylpyrimidin-2-amine (**2e** and **2k**), were highly potent against K562. The identity of R₂ as a methyl or chloro group did not affect the potency (**2a** vs **2g** and **2e** vs **2k**). The compounds with a difluoro-indene scaffold (**3a–3e**), except for **3c–3e**, were potent inhibitors of the proliferation of K562.

To evaluate the cellular activity of these compounds toward BCR-ABL^{T315I}, we employed BaF3 cells engineered to express T315I-mutated BCR-ABL. As shown in Table 1, the designed cyclic compounds **3a** and **3b** with the difluoro-indene scaffold demonstrated comparable potencies to that of ponatinib in regard to inhibiting the proliferation of BaF3 expressing BCR-ABL^{T315I}, whereas the other compounds (**1a**, **1b**, and **2a–2k**) were much less potent. The results indicated that keeping the diarylamide fragment had a very important effect on the biological activity. The potencies of the difluoro-indene scaffold compounds against BCR-ABL^{T315I} were greatly reduced both when the methyl on the phenyl group in the A region was changed to a hydrogen (**3c** and **3d**) and when *N*-methyl piperazine was translocated to the adjacent position of the difluoro group (**3e**). The structure–activity relationship (SAR) studies revealed that the phenyl group of the A region is essential for the potency. Interestingly, the effect of the methyl group on the phenyl ring on the activity is similar to that in the ponatinib derivatives. In addition, the SAR results disclosed that the amide of the B region is necessary for potent activity, and the difluoro-indene scaffold is a favored moiety for strong *in vitro* potencies.

Based on both the racemic compounds **3a** and **3b**, which displayed exceptionally high inhibitory activities, further efforts were focused on investigating the relationship between the configuration and activity due to the fact that chirality is of great importance in modern drug development. First, we sought a facile method to chemically resolve the compounds **3a** and **3b** and explored the biological properties of the pure stereoisomers. We separated the enantiomers with chiral supercritical fluid chromatography (SFC) and then assessed their cellular activity using BCR-ABL-positive CML cells (K562 and Ku812), BCR-ABL-negative CML cells (U937 and JURKAT), and BaF3 cells expressing either native or T315I mutated BCR-ABL. Four FDA-approved BCR-ABL inhibitors

Table 1. Inhibitory Activities of Compounds Against K562 and BaF3 (BCR-ABL^{T315I}) Cellular Proliferation^a

Compds.	R ₁	R ₂	R ₃	K562 Cell viability ^b (% live cells vs control)	BaF3 (BCR-ABL ^{T315I}) Cell viability ^b (% live cells vs control)
1a		-		12.0	84.3
1b		-		11.3	91.9
2a		Me		11.3	84.5
2b		Me		90.0	109.7
2c		Me		93.1	88.9
2d		Me		88.6	96.5
2e		Me		10.8	90.4
2f		Me		66.8	94.1
2g		Cl		10.1	94.5
2h		Cl		98.7	97.4
2i		Cl		82.4	74.8
2j		Cl		99.9	100.2
2k		Cl		11.0	104.8
3a		Me		9.5	1.0
3b		Me		4.3	4.9
3c		H		81.8	102.4
3d		H		80.2	114.7
3e				88.1	91.5
Ponatinib				10.1	2.8
Control				100	100

^aThe tested concentration of the compounds was 100 nM. ^bThe data represent the mean values of three independent experiments.

(imatinib, nilotinib, dasatinib, and ponatinib) were included for comparison. As expected, imatinib, nilotinib, and dasatinib were effective toward native BCR-ABL but not BCR-ABL^{T315I}

(Table 2). The (*S*)-enantiomers of **3a** (**3a-P1**) and **3b** (**3b-P1**) were more potent against cells expressing native or T315I-mutated BCR-ABL than the racemic mixtures, whereas the (*R*)-enantiomers (**3a-P2** and **3b-P2**) displayed even weaker activities than the racemic mixtures. In particular, compared with **3b-P1** and even ponatinib, **3a-P1** demonstrated a higher potency against the cells harboring native or T315I-mutated BCR-ABL and a weaker activity toward BCR-ABL-negative human leukemia cells. The results suggest that **3a-P1** possesses not only an improved potency but also an improved selectivity compared to those of ponatinib.

To understand the variation in the activity profile of the pure enantiomers **3a-P1** (*S*) and **3a-P2** (*R*), we performed a docking study (Figure 3). The predicted binding models showed that the conformations of **3a-P1** and **3a-P2** were similar in the protein binding pocket except for the difluoroindene and the *N*-methylpiperazine moieties (Figure 3B). The imidazo[1,2-*b*]pyridazine core and the amide group of **3a-P1** and **3a-P2** could both form four hydrogen bond interactions with Met318, Met290, Glu286, and Asp381 (Figure 3C and 3D). The phenyl and “flag-methyl” moieties of **3a-P1** and **3a-P2** could make favorable van der Waals interactions with the gatekeeper Ile315. Although the difluoroindene moiety and the *N*-methylpiperazine group of **3a-P1** and **3a-P2** could bind into the hydrophobic pocket, the difluoroindene moiety of **3a-P1** could form more van der Waals interactions with Ile293 and Leu354 (Figure 3D). The results of the predicted binding modes suggested that **3a-P1** could bind more tightly to the hydrophobic pocket, which is formed by the P-loop, the DFG motif, and the catalytic loop.

We further investigated the effects of **3a-P1** and ponatinib on the cell death of K562 and BaF3/BCR-ABL^{T315I} (Figure 4). The results showed that treatment with **3a-P1** and ponatinib caused similar levels of cell death in K562 (IC₅₀ ~ 10 nM). Compared with ponatinib, **3a-P1** was more effective at killing BaF3/BCR-ABL^{T315I} cells.

To further confirm the target inhibition in cells expressing native or T315I-mutated BCR-ABL, we examined the effect of **3a-P1** on the tyrosine phosphorylation status of BCR-ABL and the direct BCR-ABL substrate CRKL using Western blotting assays (Figure 5). The results showed that **3a-P1** and ponatinib demonstrated similar activities against the phosphorylation of BCR-ABL in K562 and BaF3 expressing native and T315I-mutated BCR-ABL. Notably, **3a-P1** seemed to be more potent at inhibiting CRKL phosphorylation than ponatinib.

As compound **3a-P1** demonstrated a potent antitumor activity and the clear target inhibition on T315I-mutated BCR-ABL, **3a-P1** was subsequently characterized using mouse pharmacokinetic (PK) studies before the *in vivo* efficacy investigation was conducted (Table 3). When intravenously administered at a dose of 5 mg/kg in mice, compound **3a-P1** displayed a slower clearance rate than that of ponatinib. When orally administered at a dose of 15 mg/kg, the oral exposure of **3a-P1** was higher than that of ponatinib. The oral bioavailability of compound **3a-P1** was determined to be 32%. Moreover, the elimination half-life of **3a-P1** was longer than that of ponatinib. Taken together, its good oral bioavailability and ideal half-life suggested that **3a-P1** may have good efficacy *in vivo* when orally administered and may be more potent *in vivo* than ponatinib at the same dose.

Based on the promising *in vitro* findings combined with the excellent *in vivo* PK profiles of **3a-P1**, we conducted experiments to determine the *in vivo* antitumor potency of

Table 2. Effect of BCR-ABL Inhibitors on the Cell Viability of BCR-ABL-Positive and BCR-ABL-Negative Leukemia Cell Lines and a Panel of BaF3 Cell Transfectants (IC_{50} as the Mean \pm SEM (nM))^a

compounds	BaF3 cells		CML cells		non-CML cells	
	native BCR-ABL	T315I BCR-ABL	K562	Ku812	U937	JURKAT
imatinib	>100	>100	82.9 \pm 11.2	51.3 \pm 4.3	>1000	>1000
nilotinib	11.8 \pm 0.4	>100	1.8 \pm 0.4	1.8 \pm 0.1	>1000	>1000
dasatinib	0.7 \pm 0.1	>100	0.2 \pm 0.1	0.1 \pm 0.1	>1000	>1000
ponatinib	0.9 \pm 0.1	9.6 \pm 1.7	0.3 \pm 0.1	0.1 \pm 0.1	245.8 \pm 12.5	295.0 \pm 5.0
3a	2.7 \pm 0.2	11.0 \pm 0.2	0.5 \pm 0.1	0.2 \pm 0.1	607.8 \pm 42.2	672.4 \pm 77.6
3a-P1	2.1 \pm 0.2	4.7 \pm 1.3	0.4 \pm 0.1	0.1 \pm 0.1	867.6 \pm 88.7	850.7 \pm 25.7
3a-P2	31.2 \pm 3.8	>100	3.6 \pm 0.1	2.7 \pm 0.1	>1000	>1000
3b	9.3 \pm 2.5	40.0 \pm 9.6	1.0 \pm 0.2	0.4 \pm 0.1	190.8 \pm 3.3	292.0 \pm 8.0
3b-P1	3.5 \pm 0.9	12.4 \pm 0.4	0.6 \pm 0.1	0.2 \pm 0.1	165.0 \pm 15.0	280.0 \pm 20.0
3b-P2	62.5 \pm 6.9	>100	10.4 \pm 1.5	5.2 \pm 0.2	465.3 \pm 9.7	399.9 \pm 64.9

^aThe data represent the mean values of three independent experiments.

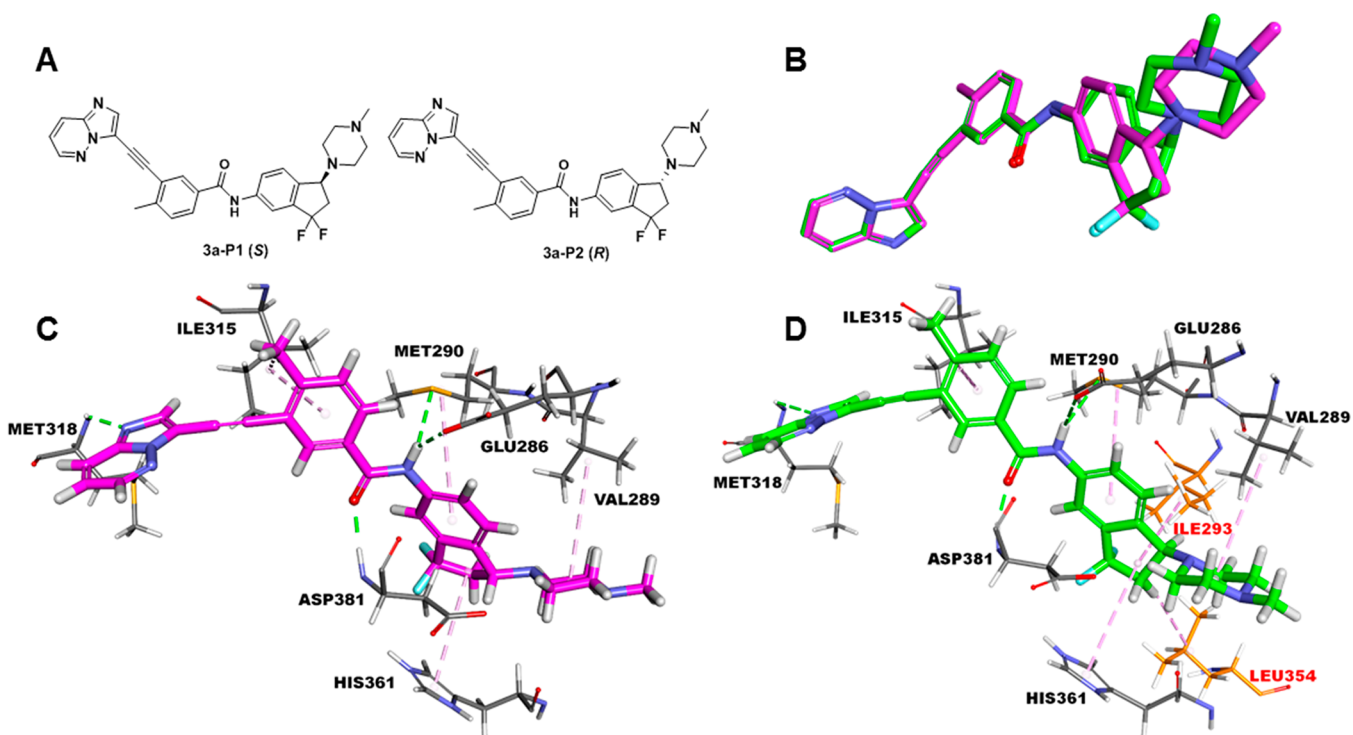


Figure 3. (A) Structures of 3a-P1 and 3a-P2. (B) Overlays of the docked poses of 3a-P1 and 3a-P2 with the BCR-ABL^{T315I} mutant kinase (PDB 3IK3). (C) The predicted binding modes of 3a-P2 with the BCR-ABL^{T315I} mutant kinase (PDB 3IK3). (D) The predicted binding modes of 3a-P1 with the BCR-ABL^{T315I} mutant kinase (PDB 3IK3). 3a-P1 is shown in green, 3a-P2 is shown in pink, hydrogen bonds are shown as green dashed lines, and van der Waals interactions are shown as magenta dashed lines.

3a-P1 in a subcutaneous xenograft model of BaF3 expressing T315I-mutated BCR-ABL. Considering that ponatinib was approved as its hydrochloride salt, we synthesized the hydrochloride of 3a-P1 to evaluate its *in vivo* efficacy. As shown in Figure 6A, ponatinib in its hydrochloride salt inhibited tumor growth, with a tumor growth inhibition (TGI) of 53% based on daily oral dosing at 5 mg/kg. Compared with the vehicle control, daily oral dosing of 2.5, 5, and 10 mg/kg of 3a-P1·HCl caused a reduction in mean tumor volumes at the final measurements, with TGI values of 69%, 87% and 107%, respectively, showing an obvious dose–effect relationship. Notably, 3a-P1·HCl demonstrated a higher activity in terms of suppressing tumor growth than that of ponatinib, as treatment with 3a-P1·HCl at 2.5 mg/kg per day achieved a similar TGI level to that of ponatinib at a higher dose (5 mg/kg). 3a-P1·

HCl likely could achieve a TGI of more than 100% at 10 mg/kg per day. It is noteworthy that no obvious effect on the mouse body weight was observed for 15 days of treatment (Figure 6B).

Given its highly potent *in vitro* and *in vivo* antiproliferative activities, we further investigated the preliminary druggability profile of compound 3a-P1 (Table 4). In a hERG inhibition assay, compound 3a-P1 showed hERG channel activity with an IC_{50} value of 11.1 μ M that was lower than that of ponatinib (IC_{50} = 8 μ M), which indicates that it had less potential for cardiotoxicity. We also studied its mutagenicity using a bacterial reverse mutation (Ames) test. Compound 3a-P1 was nonmutagenic at the tested concentrations (0.5–312.5 μ g per plate) with or without metabolic activation (using the five *Salmonella typhimurium* test strains TA97a, TA98, TA100,

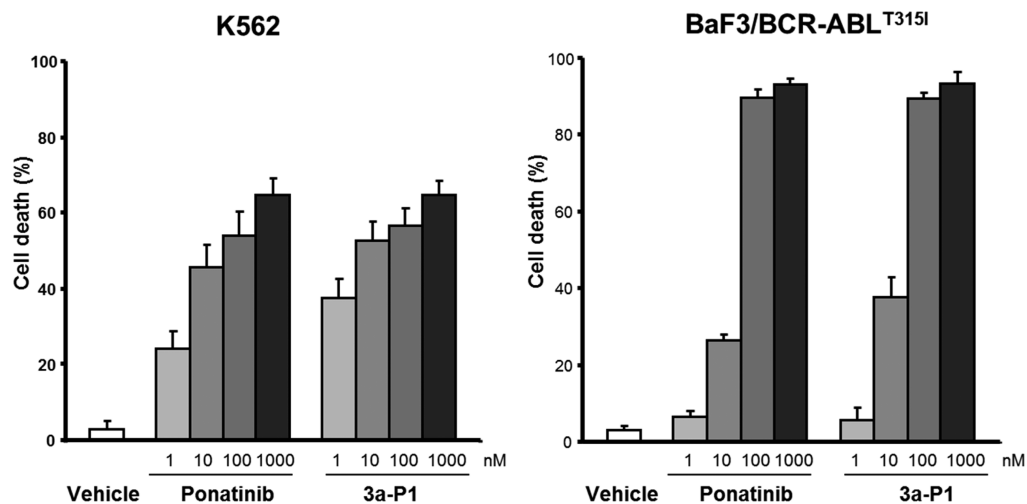


Figure 4. Effect of 3a-P1 and ponatinib on the cell death of K562 and BaF3/BCR-ABL^{T3151}.

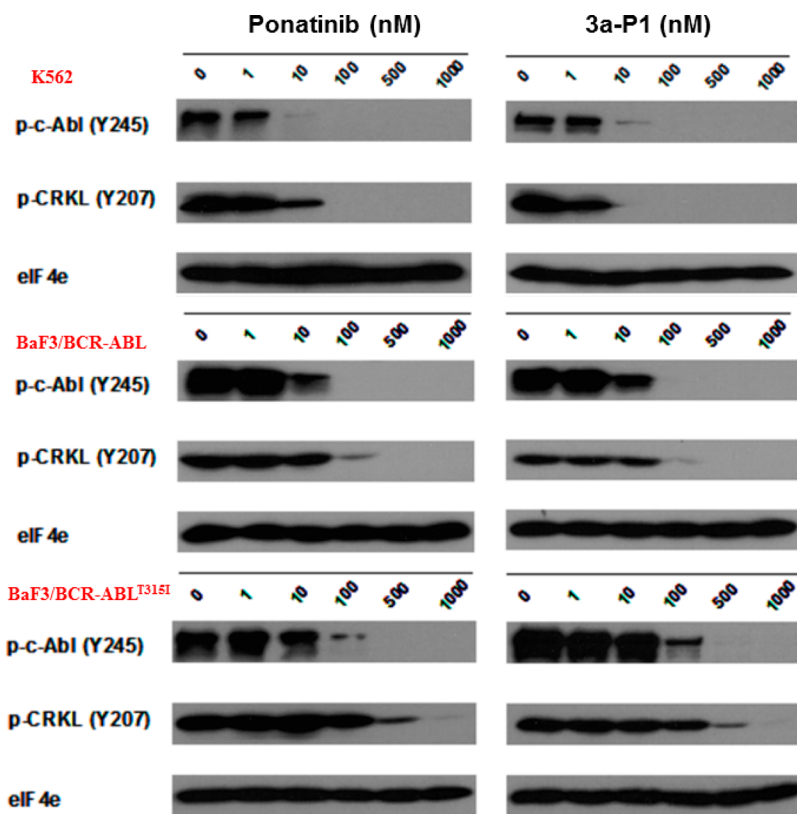


Figure 5. Effect of 3a-P1 and ponatinib on the inhibition the phosphorylation of ABL and ABL^{T3151}. K562, BaF3/BCR-ABL, and BaF3/BCR-ABL^{T3151} cells were treated with ponatinib and 3a-P1 at the indicated concentrations. After 4 h of treatment, cells were harvested, lysed, and analyzed by immunoblots using an antibody for either phosphorylated BCR-ABL (Y245) or CRKL (Y207). eIF 4e was employed as an internal control.

Table 3. Pharmacokinetic Parameters Following Intravenous and Oral Dosing in ICR Mice^a

compounds	route	T_{max} (h)	C_{max} (ng/mL)	AUC_{0-t} (h·ng/mL)	$AUC_{0-\infty}$ (h·ng/mL)	MRT (h)	$T_{1/2}$ (h)	CL (L/h per kilogram)	V_{ss} (L/kg)	F (%)
3a-P1	po (15 mg/kg)	5.0	129	1386	1443	8.22	4.61			32
	iv (5 mg/kg)	0.08	1470	1389	1502	5.11	5.30	3.72	18.1	
ponatinib	po (15 mg/kg)	1.5	70.0	363	432	5.25	2.84			27
	iv (5 mg/kg)	0.08	270	497	528	4.29	3.28	9.68	41.0	

^aOral (po) and intravenous (iv); $n = 4$ animals per study (po) and $n = 3$ animals per study (iv).

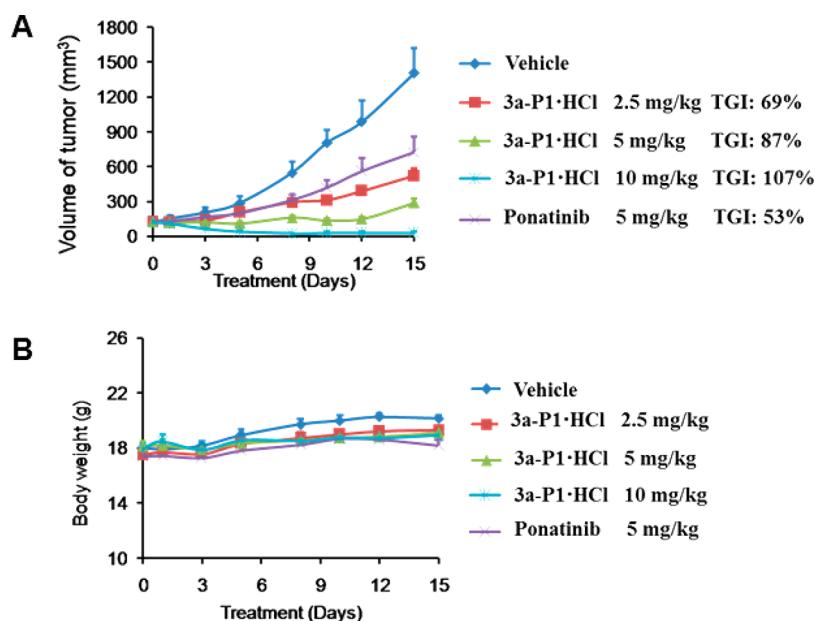


Figure 6. Efficacy of 3a-P1 and ponatinib in mouse subcutaneous xenograft models driven by BCR-ABL^{T315I}. (A) Mice bearing BaF3/BCR-ABL^{T315I} xenografts were orally treated once daily with either a vehicle or the indicated doses of 3a-P1·HCl and ponatinib. (B) Changes in mice body weight after treatment with 3a-P1 and ponatinib. Results are expressed as the mean tumor volume \pm SD ($n = 10$ for each group in panel A). TGI stands for tumor growth inhibition. A TGI larger than 100% indicates that tumors treated with the drugs are smaller than their original sizes.

Table 4. Safety Profile of Compound 3a-P1

compound	hERG K ⁺ inhibition			single-dose toxicity ^d		
	IC ₅₀ (μ M)	Ames ^a	chromosome aberration ^b	mice bone marrow micronucleus ^c	ICR mice, MTD (mg/kg)	
3a-P1	11.1	negative	negative	negative	100	

^aCompound 3a-P1 was tested from 0.5 to 312.5 μ g/plate with or without metabolic activation using the five *Salmonella typhimurium* test strains TA97a, TA98, TA100, TA102, and TA1535; 3a-P1·HCl was used. ^bDoses were as follows: 0.563, 1.125, 2.25, and 4.5 μ g/mL; 3a-P1·HCl was used. ^cDoses were as follows: 25, 50, and 100 mg/kg; 3a-P1·HCl was used. ^dMice were observed for 14 d after a single-dose oral administration; 3a-P1·HCl was used.

TA102, and TA1535). In the chromosome aberration and mouse bone marrow micronucleus assays, compound 3a-P1 was also found to be negative. A mice single-dose toxicity study was also performed for compound 3a-P1, and the maximum tolerated dose was determined to be 100 mg/kg.

Finally, to further understand its kinase selectivity, the inhibitory activities of compound 3a-P1 against different ABL kinases and other kinases were evaluated. As depicted in Figure 7, both 3a-P1 and ponatinib exhibited strong and similar inhibitory effects on human ABL kinase and its mutants, resulting in only 0.1%–6% of the kinase activity remaining compared with the DMSO control group shown in the enlarged segment. In particular, for the mutant T315I, the inhibition of 3a-P1 and ponatinib both reached about 95% at the tested concentration of 10 nM. Additionally, the IC₅₀ values of 3a-P1 for the c-Kit and TIE2/TEK kinases were predicted to be about 10 nM. By comparison, the IC₅₀ values of 3a-P1 for c-Src, FGFR1, FLT3, KDR/VEGFR2, LYN, and PDGFR α kinases were all less than 10 nM. These results illustrated that compound 3a-P1 may be useful for the treatment of CML as well as other solid tumors, such as triple-negative breast cancers.

CHEMISTRY

Synthetic route of urea compounds 1a and 1b is schematically illustrated in Scheme 1. First, the key intermediates 6a and 6b were prepared from commercially available compounds 4a and

4b. Second, compound 7 was coupled with compounds 6a and 6b under Sonogashira coupling conditions, followed by deprotection to yield compounds 9a and 9b, respectively. Finally, the target compounds 1a and 1b were obtained through a condensation reaction between intermediates 9a or 9b, respectively, and 10. Compound 10 was prepared according to the reported methods.⁹

The preparation of benzimidazole compounds 2a–e and 2g–k is illustrated in Scheme 2. The starting material 3,4-dinitrobenzoic acid (11) reacted with *N*-methyl piperazine to afford compound 12, which was then reduced to give intermediate 13. The reduction of the nitro group of compound 13 by catalytic hydrogenation afforded compound 14. The benzimidazole core structure was constructed by reacting compound 14 with the iodide-substituted benzoic acids (15a and 15b). Finally, compounds 16a and 16b were coupled with aryl alkynyl compounds (17a–e) under Sonogashira coupling conditions to deliver the final products 2a–e and 2g–k.

The synthetic procedure for compound 2f is briefly described in Scheme 3. The starting material 18 was coupled with imidazole to afford compound 19, which was converted to the benzimidazole core structure by sequential reduction and condensation reactions. Finally, the target compound 2f was obtained by the Sonogashira coupling reaction of iodide intermediate 22 and the aryl alkynyl compound 17a.

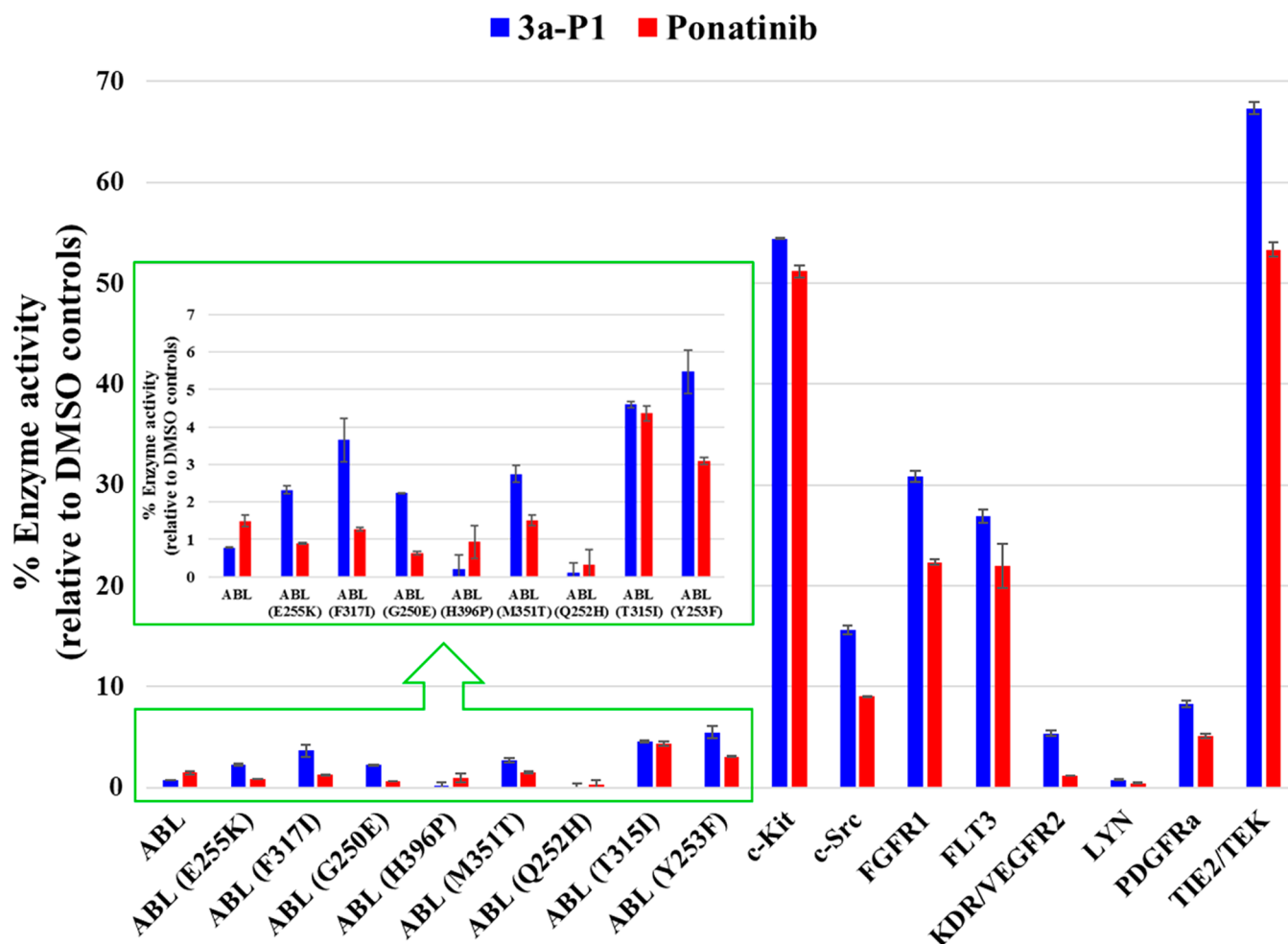
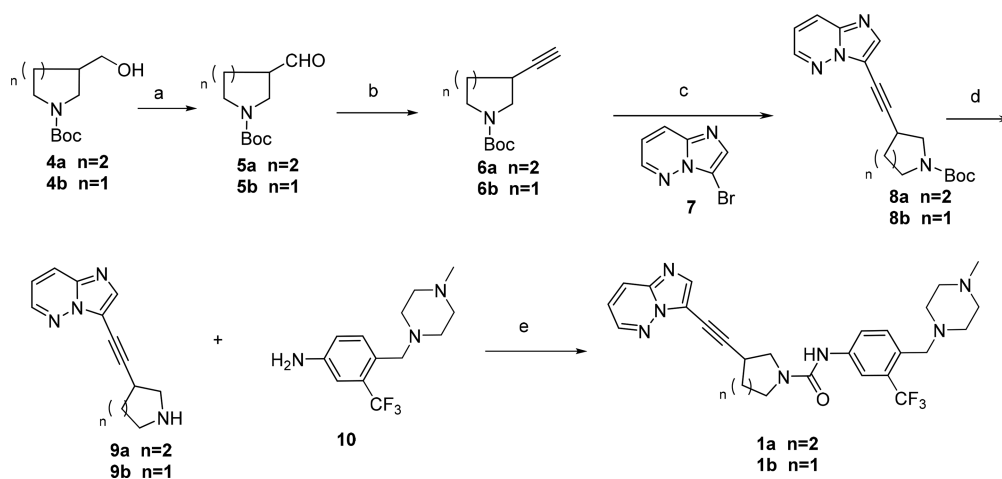


Figure 7. Kinase inhibition profiles of compound 3a-P1 and ponatinib for native ABL, different mutants, and selected kinases at 10 nM.

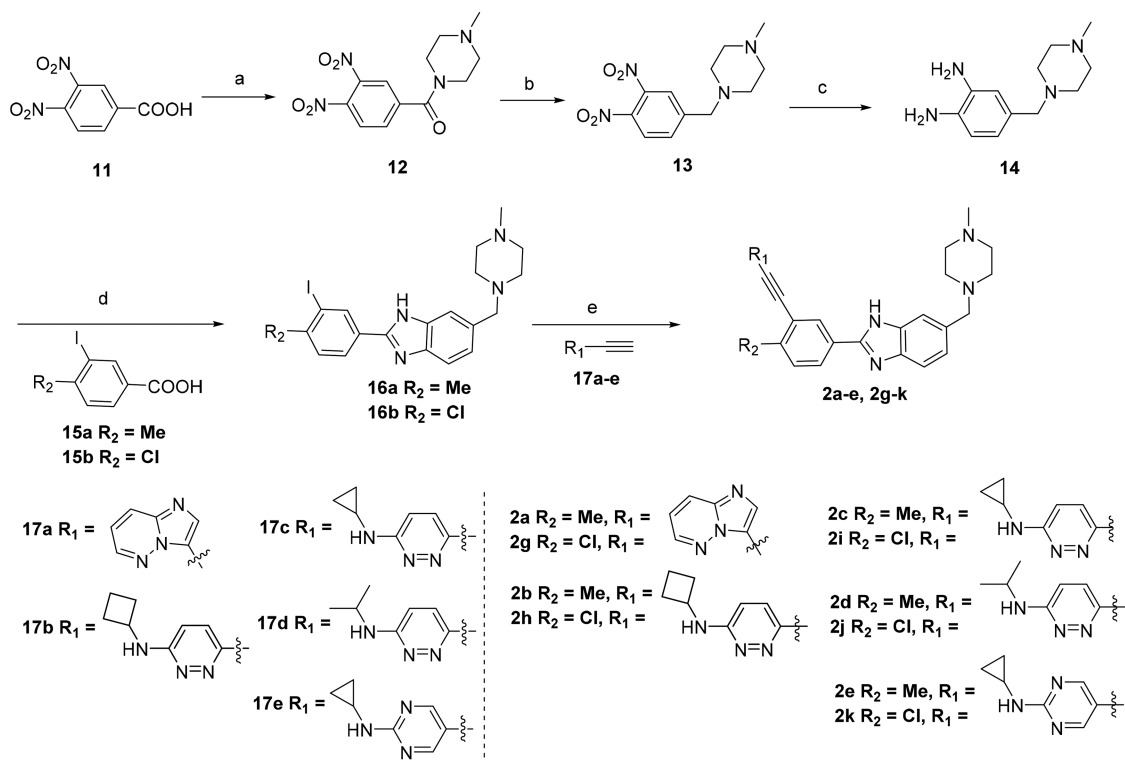
Scheme 1. Synthesis of Compounds 1a and 1b⁴



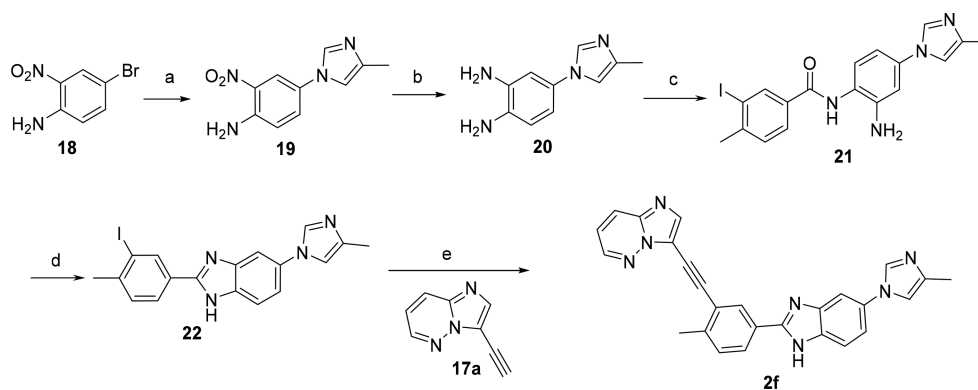
^aReagents and conditions are as follows: (a) pyridine·SO₃, DMSO, rt, 2 h, 69–70%; (b) (diazomethyl)phosphonic acid dimethyl ester, K₂CO₃, MeOH, 0 °C to rt, overnight, 100–101%; (c) Pd(PPh₃)₂Cl₂, CuI, DIPEA, DMF, 80 °C, Ar₂, 6 h, 60–61%; (d) TFA, CH₂Cl₂, overnight, rt, 107–108%; and (e) 4-nitrophenyl chloroformate, pyridine, dioxane, 60 °C, 11 h, 19–32%.

The designed difluoro-indene compounds 3a–e were prepared using a palladium-catalyzed Sonogashira coupling reaction as the key step (Scheme 4). Briefly, the key intermediate 23 was synthesized according to our reported method using commercially available 2,3-dihydro-1H-inden-1-

one as the starting material.¹⁷ The following reduction of the NO₂ group afforded the amine intermediate 24, which was reacted with the substituted benzoic acids (15a and 15b) to give the amide intermediates 25a and 25b, respectively. Compounds 25a and 25b were converted to the target

Scheme 2. Synthesis of Compounds 2a–e and 2g–k^a

^aReagents and conditions are as follows: (a) (i) SOCl₂, reflux, 6 h, (ii) *N*-methylpiperazine, Et₃N, 5 °C to rt, CH₂Cl₂, overnight, 95%; (b) NaBH₄, BF₃·OEt₂, 5 °C to rt, THF, 5 h, 80%; (c) 10% Pd/C, H₂, DMF/MeOH = 1:1, 12 h; (d) (i) EDCl, HOBT, DMF, rt, 24 h, (ii) AcOH, reflux, 3 h, 30–43%; and (e) Pd(PPh₃)₄, CuI, DIPEA, DMF, rt, Ar₂, 20 h, 9–78%.

Scheme 3. Synthesis of Compound 2f^a

^aReagents and conditions are as follows: (a) K₂CO₃, CuI, 8-hydroxyquinoline, 4-methylimidazole, DMSO, sealed tube, 120 °C, Ar₂, 29 h, 57%; (b) Raney Ni, H₂, rt, 7 h, 96%; (c) (i) 3-iodo-4-methylbenzoic acid, SOCl₂, reflux, 2 h, (ii) Et₃N, DMAP, rt, THF, 20 h, 37%; (d) AcOH, reflux, 8 h, 65%; and (e) Pd(PPh₃)₄, CuI, DIPEA, DMF, rt, 20 h, 63%.

compounds 3a–d via a Sonogashira coupling reaction. Compound 3e was prepared from compound 26, which was prepared according to our published method,¹⁷ by a similar procedure.

Enantiomerically pure 3a and 3b isomers were prepared via supercritical fluid chromatography resolution through a chiral stationary phase (Scheme 5). Racemates 3a and 3b were cleanly separated into the optically pure enantiomers 3a-P1 and 3a-P2 and 3b-P1 and 3b-P2, respectively.

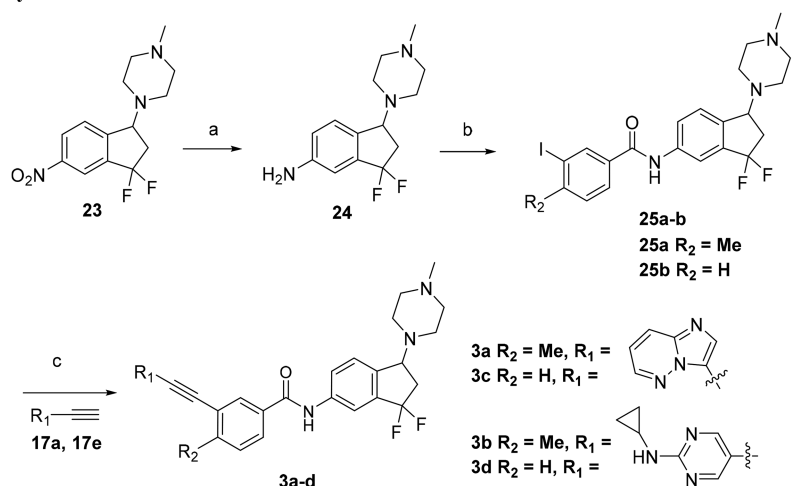
To determine the absolute configuration of the above prepared compounds by SFC, we synthesized the optical pure chiral compound 3a from the chiral isomer of compound 23

(Scheme 6). The key chiral compound (*S*)-23 was prepared by the chiral resolution of 23, and *D*-camphorsulfonic acid was used as the chiral resolving agent. Compound 3a-P1 was synthesized from compound (*S*)-23 by procedures similar to those shown in Scheme 4.

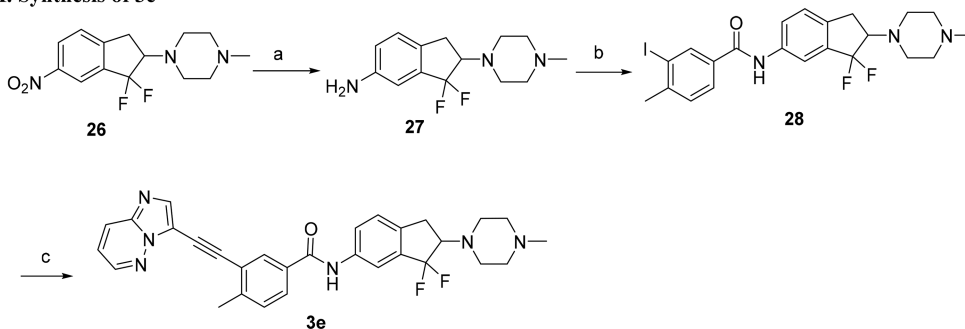
The absolute configuration of the synthesized compound (*S*)-23, which was dissociated from the *D*-camphorsulfonic salt of 29, was determined by comparing the experimental ECD spectrum of compound (*S*)-23 and the corresponding calculated ECD spectra of the optical isomers (*S*)-23 and (*R*)-23. The ECD spectrum recorded for (*S*)-23 matched the calculated ECD curve of (*S*)-23 well but was opposite to that

Scheme 4. Synthesis of Compounds 3a–e^a

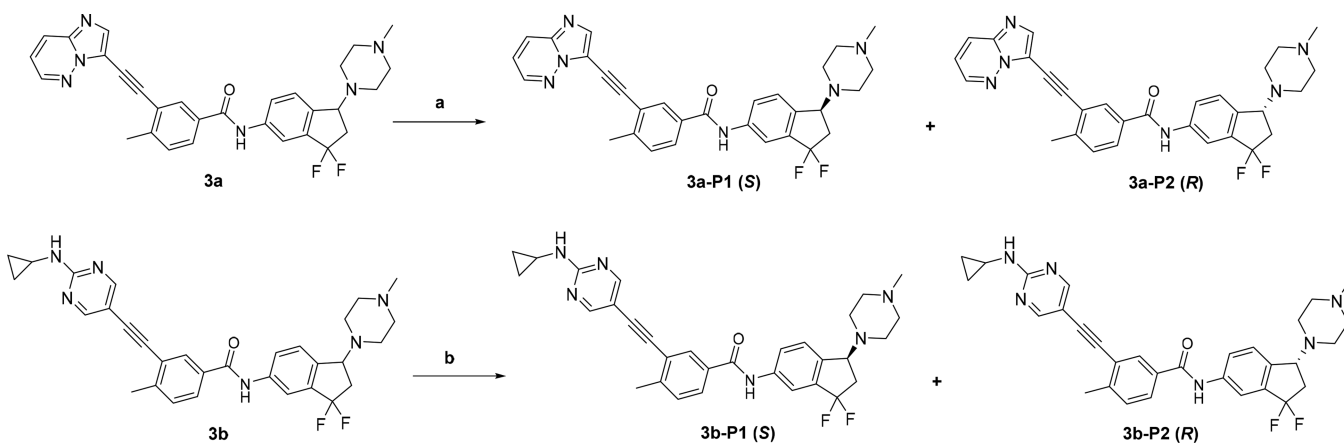
I. Synthesis of 3a–d



II. Synthesis of 3e



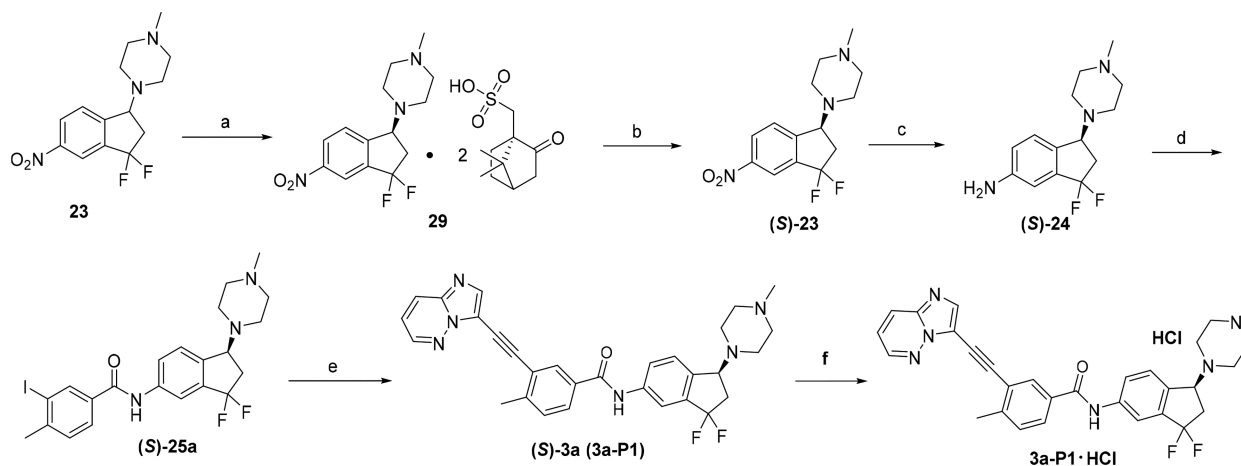
^aReagents and conditions are as follows: (a) 10% Pd/C, H₂, MeOH, 12 h; (b) (i) substituted benzoic acids, SOCl₂, reflux, 6 h, (ii) Et₃N, DMAP, rt, THF, overnight, 51–92%; and (c) Pd(PPh₃)₄, CuI, DIPEA, DMF, rt, 20 h, 5–30%.

Scheme 5. Separation of the Optical Isomers of Compounds 3a and 3b^a

^aReagents and conditions are as follows: (a) CHIRALCEL AS-H, CO₂/MeOH (0.1% diethyl amine) = 60:40 (v/v) and (b) CHIRALCEL OJ-H, CO₂/EtOH (0.1% diethyl amine) = 75:25 (v/v).

of (*R*)-23 (Figure 8A). Moreover, the calculated UV spectrum of (*S*)-23 displayed a curve similar to the experimental UV spectrum of (*S*)-23 (Figure 8B). Therefore, the synthesized compound (*S*)-23 was deduced to have the (*S*) absolute configuration. Furthermore, the single crystal of compound 29 was obtained and characterized by X-ray diffraction. The crystal structure of compound 29 is depicted in Figure 9. Two

molecules of *D*-camphorsulfonic acid were bound with one molecule of compound 29, and the absolute configuration of 29 was (*S*). Thus, the absolute configuration of (*S*)-23 was confirmed as the (*S*)-configuration. The absolute configurations of compounds 3a-P1 and 3a-P2, respectively, were determined comparing the experimental ECD spectra. The experimental ECD spectrum of 3a-P1 displayed a CD diagram

Scheme 6. Synthesis of Compounds 3a-P1 and 3a-P1·HCl^a

^aReagents and conditions are as follows: (a) D-camphorsulfonic acid, MeOH/*i*PrOH = 1:2, reflux to rt, 32%; (b) NaOH, H₂O, rt, 100%; (c) 10% Pd/C, H₂, MeOH, 12 h, 95%; (d) (i) SOCl₂, reflux, 1 h; (ii) Et₃N, DMAP, rt, THF, overnight, 69%; (e) Pd(PPh₃)₄, CuI, DIPEA, DMF, rt, 20 h, 37%; and (f) acetone, 1 M HCl in EtOH, rt, 6 h, 102%.

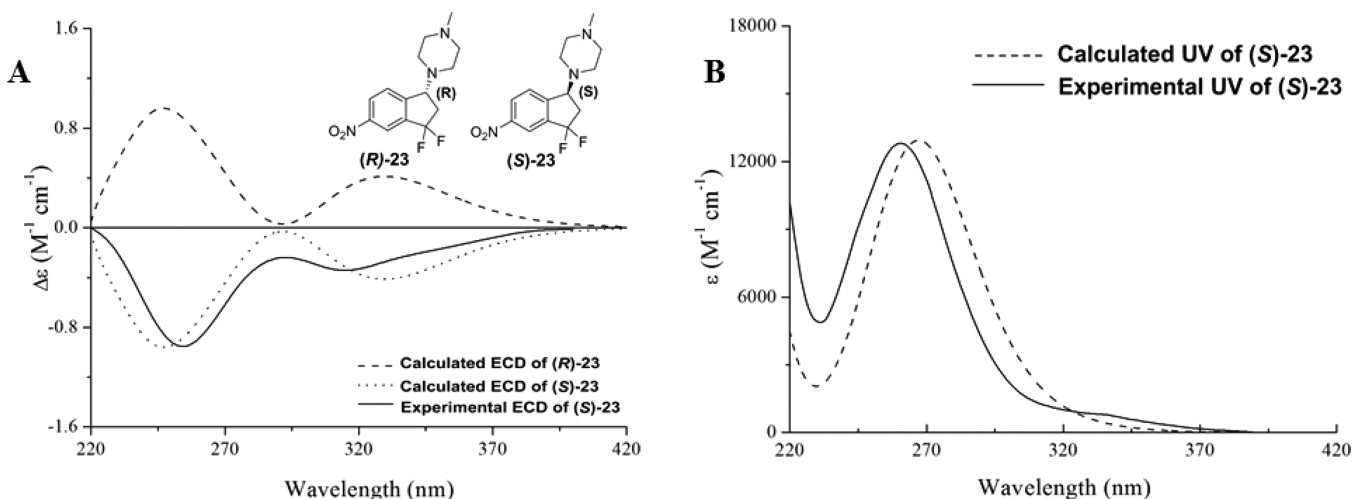


Figure 8. (A) Calculated and experimental ECD spectra of compounds (R)-23 and (S)-23. (B) Calculated and experimental UV spectra of compound (S)-23.

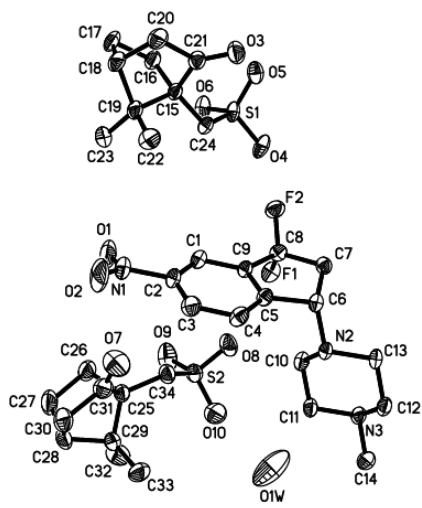


Figure 9. X-ray crystallographic structure of 29.

similar to the experimental spectrum of (S)-3a (Figure 10). Therefore, compound 3a-P1 was elucidated to have the (S) absolute configuration, and 3a-P2 was elucidated to have (R) absolute configuration. The absolute configurations of 3b-P1 and 3b-P2 were consistent with those of 3a-P1 and 3a-P2, respectively, according to the same rotation.

CONCLUSION

In summary, we have identified a novel difluoro-indene derivative 3a-P1 in the (S)-configuration as a highly potent BCR-ABL inhibitor that displays significant activities against a broad spectrum of BCR-ABL mutants, including the gate-keeper T315I mutant, through a structure-based medicinal chemistry optimization strategy. Additionally, 3a-P1 showed potent inhibition against the kinases c-KIT, TIE2/TEK, c-Src, FGFR1, FLT3, KDR/VEGFR2, LYN, and PDGFRα. The results provide a strong rationale for the potential evaluation of 3a-P1 in CML and a range of other cancers driven by multiple tyrosine kinases such as c-KIT. The PK profile of compound 3a-P1 was also favorable, and its exposure value in ICR mice was higher than that of ponatinib. In particular, 3a-P1

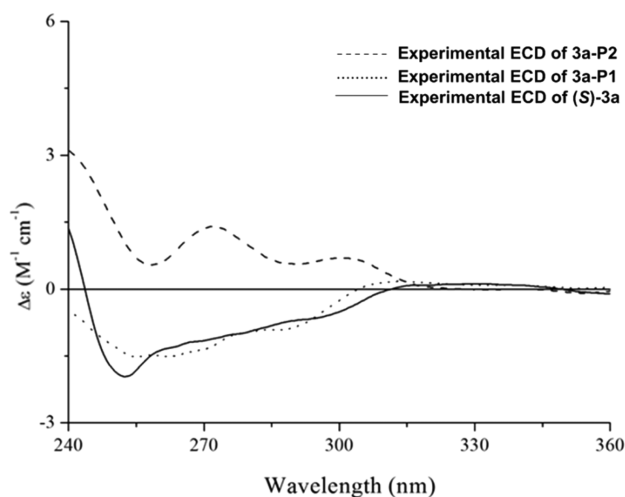


Figure 10. Experimental ECD spectra of compounds **3a-P1**, **3a-P2**, and **(S)-3a**.

demonstrated a higher potency than that of ponatinib in a mice xenograft model of BaF3 expressing BCR-ABL^{T315I}. Furthermore, a panel of safety assessments, including a hERG K⁺ channel inhibition assay, an Ames test, chromosome aberration and mice bone marrow micronucleus assays, and acute toxicity studies, demonstrated that **3a-P1** displayed an acceptable safety profile for further characterization. Overall, these pharmacological and safety data have laid a solid foundation to develop **3a-P1** as a promising drug candidate.

EXPERIMENTAL SECTION

Chemistry. ¹H NMR spectra were obtained on a Varian mercury spectrometer at 300 or 400 MHz in CDCl₃, DMSO-*d*₆, or CD₃OD. Chemical shifts and coupling constants are recorded in units of parts per million and hertz, respectively. Melting points were determined on a Yanaco MP-J3 melting point apparatus. High-resolution mass spectra were recorded on an Agilent 1100 series LC/MSD trap mass spectrometer (ESI-TOF). All target compounds were purified by chromatography and have purities of ≥95% as determined by HPLC/MS analyses conducted on an Agilent 1100 system using a reversed-phase C18 column with 75% CH₃CN in water (0.1% HCOOH) and a flow rate of 0.4 mL/min. All reagents and solvents were purchased from commercial sources unless otherwise indicated. Thin layer chromatography was carried out on silica gel plates (GF254), and components were visualized by either UV light (254 nm) or exposure to I₂. Column chromatography was carried out on silica gel (300–400 mesh).

Synthesis of Compounds 1a and 1b. **1-Boc-3-formylpiperidine (5a).** 1-Boc-3-hydroxymethylpiperidine **4a** (2.15 g, 10 mmol) and triethylamine (3.03 g, 30 mmol) were dissolved in 10 mL of DMSO. To the mixture was added 15 mL of a DMSO solution of Py-SO₃ (4.77 g, 30 mmol) dropwise, and the result mixture was stirred at rt for 2 h. The mixture was poured into 100 mL of ice–water and extracted with EtOAc (100 mL × 3). The organic layer was washed with brine, dried with Na₂SO₄, and filtered, and the filtrate was evaporated in a vacuum. The crude product was purified by chromatography on silica gel (PE/EtOAc 5:1) to give 1.46 g of the product as colorless oil (69%). ¹H NMR (300 MHz, CDCl₃): δ 9.70 (1 H, s), 3.93–3.91 (1 H, m), 3.67–3.62 (1 H, m), 3.36–3.29 (1 H, m), 3.13–3.05 (1 H, m), 2.45–2.40 (1 H, m), 1.97–1.95 (1 H, m), 1.72–1.63 (2 H, m), 1.59–1.49 (1 H, m), 1.46 (9 H, s).

1-Boc-3-ethynylpiperidine (6a). A solution of compound **5a** (1.46 g, 6.85 mmol) and (diazomethyl) phosphonic acid dimethyl ester (1.79 g, 11.94 mmol) in 50 mL of methanol was stirred at 0 °C for 10 min. To the mixture was added K₂CO₃ (1.96 g, 14.2 mmol). The mixture was stirred at 0 °C for 2 h, then stirred at rt overnight. The

mixture was evaporated in a vacuum. To the residue were added EtOAc and water. The organic layer was separated, and the water layer was extracted with EtOAc (100 mL × 3). The combined organic layers were successively washed with water and brine, dried with Na₂SO₄, and filtered, and the filtrate was evaporated in a vacuum to give 1.44 g of the product as colorless oil (100%). ¹H NMR (300 MHz, CDCl₃): δ 3.90 (1 H, brs), 3.75–3.70 (1 H, m), 3.02–2.95 (2 H, m), 2.47–2.40 (1 H, m), 2.05 (1 H, d, *J* = 2.1 Hz), 1.99–1.94 (1 H, m), 1.73–1.69 (1 H, m), 1.63–1.50 (2 H, m), 1.46 (9 H, s).

1-Boc-3-(2-(imidazo[1,2-*b*]pyridazin-3-yl)ethynyl)piperidine (8a). A solution of compound **6a** (0.55 g, 2.6 mmol), 3-bromoimidazo[1,2-*b*]pyridazine **7** (0.40 g, 2 mmol), Pd(PPh₃)₂Cl₂ (70 mg, 0.1 mmol), CuI (29 mg, 0.15 mmol), and DIPEA (0.39 g, 3 mmol) in DMF (20 mL) was stirred at 80 °C under Ar₂ for 6 h. The mixture was poured into 100 mL of water and extracted with EtOAc (60 mL × 3). The organic layer was washed with brine, dried with Na₂SO₄, and filtered, and the filtrate was evaporated in a vacuum. The crude product was purified by chromatography on silica gel (PE/EtOAc = 7:3 to 3:2) to give 0.39 g of the product as yellow oil (60%). ¹H NMR (300 MHz, CDCl₃): δ 8.50 (1 H, d, *J* = 4.2 Hz), 8.08–7.98 (2 H, m), 7.15 (1 H, dd, *J* = 4.5 and 8.7 Hz), 4.09 (1 H, brs), 3.82–3.76 (1 H, m), 3.19 (1 H, brs), 3.09–3.02 (1 H, m), 2.88–2.81 (1 H, m), 2.32 (1 H, brs), 2.15–2.11 (1 H, m), 1.81–1.67 (2 H, m), 1.46 (9 H, s). LC-MS: *m/z* [M + H]⁺ 327.2112.

3-(2-(Imidazo[1,2-*b*]pyridazin-3-yl)ethynyl)piperidine (9a). To a solution of compound **8a** (0.39 g, 1.2 mmol) in CH₂Cl₂ (10 mL) was added TFA (1.23 g, 10.8 mmol). The mixture was stirred at rt overnight and evaporated in a vacuum. To the residue was added 10 mL of a 10% K₂CO₃ solution, and the mixture was extracted with EtOAc (20 mL × 3). The combined organic layers were washed with brine, dried with Na₂SO₄, and filtrated, and the filtrate was evaporated in a vacuum to give 0.33 g of the product as yellow oil (107%). ¹H NMR (300 MHz, CDCl₃): δ 8.43 (1 H, d, *J* = 4.5 Hz), 7.95 (1 H, dd, *J* = 1.8 and 9.0 Hz), 7.91 (1 H, s), 7.07 (1 H, dd, *J* = 4.5 and 9.0 Hz), 2.98–2.82 (4 H, m), 2.11–2.08 (1 H, m), 1.84–1.75 (2 H, m), 1.58–1.53 (2 H, m). LC-MS: *m/z* [M + H]⁺ 227.1325.

***N*-(3-(Trifluoromethyl)-4-((4-methylpiperazin-1-yl)methyl)phenyl)-3-(2-(imidazo[1,2-*b*]pyridazin-3-yl)ethynyl)piperidine-1-carboxamide (1a).** To a solution of compound **10** (0.1 g, 0.37 mmol) in 15 mL of anhydrous dioxane was added pyridine (0.036 mL, 0.45 mmol) and 4-nitrophenyl chloroformate (90 mg, 0.45 mmol). The mixture was stirred at 60 °C for 2 h and then cooled to rt, and compound **9a** (0.1 g, 0.44 mmol) was added to the above mixture. The mixture was stirred at 60 °C for 9 h and evaporated in a vacuum. The residue was purified by chromatography on silica gel (CH₂Cl₂/CH₃OH = 25:1) to give 140 mg of the crude product, and continued purification via preparation TLC (CH₂Cl₂/CH₃OH = 120:15) gave 60 mg of the product as a pale yellow solid (32%). mp: 68–70 °C. ¹H NMR (300 MHz, CDCl₃): δ 8.38 (1 H, s), 7.97 (1 H, d, *J* = 9.0 Hz), 7.88 (1 H, s), 7.61–7.58 (2 H, m), 7.43 (1 H, d, *J* = 7.8 Hz), 7.10–7.06 (1 H, m), 7.03 (1 H, s), 3.99–3.95 (2 H, m), 3.65–3.49 (5 H, m), 3.02 (4 H, brs), 2.79 (4 H, s), 2.69 (3 H, s), 2.13 (1 H, brs), 1.93 (2 H, brs), 1.63 (1 H, brs). HRMS (ESI-TOF⁺): *m/z* [M + H]⁺ calcd for C₂₇H₃₁F₃N₇O 526.2537, found 526.2536.

1-Boc-3-formylpyrrolidine (5b). In a similar manner to **5a**, compound **5b** was prepared from **4b** (1.40 g, colorless oil, 70%). ¹H NMR (300 MHz, CDCl₃): δ 9.68 (1 H, s), 3.72–3.68 (1 H, m), 3.51–3.48 (1 H, m), 3.37 (2 H, brs), 3.03–2.99 (1 H, m), 2.24–2.05 (2 H, m), 1.45 (9 H, s).

1-Boc-3-ethynylpyrrolidine (6b). In a similar manner to **6a**, compound **6b** was prepared from **5b** and (diazomethyl)phosphonic acid dimethyl ester (1.39 g, colorless oil, 101%). ¹H NMR (300 MHz, CDCl₃): δ 3.60–3.47 (2 H, m), 3.30 (2 H, brs), 2.95–2.90 (1 H, m), 2.18–2.12 (1 H, m), 2.10 (1 H, d, *J* = 1.8 Hz), 1.96–1.90 (1 H, m), 1.45 (9 H, s).

1-Boc-3-(2-(imidazo[1,2-*b*]pyridazin-3-yl)ethynyl)pyrrolidine (8b). In a similar manner to **8a**, compound **8b** was prepared from **6b** and 3-bromoimidazo[1,2-*b*]pyridazine **7** (0.38 g, yellow oil, 61%). ¹H NMR (300 MHz, CDCl₃): δ 8.43 (1 H, d, *J* = 3.6 Hz), 7.99–7.92 (2

H, m), 7.09 (1 H, dd, $J = 4.2$ and 9.0 Hz), 3.77–3.75 (1 H, m), 3.60–3.45 (4 H, m), 2.32–2.12 (2 H, m), 1.47 (9 H, s).

3-(2-(Imidazo[1,2-*b*]pyridazin-3-yl)ethynyl)pyrrolidine (9b). In a similar manner to **9a**, compound **9b** was prepared from **8b** (0.28 g, yellow oil, 108%). $^1\text{H NMR}$ (300 MHz, CDCl_3): δ 8.43 (1 H, d, $J = 4.2$ Hz), 7.95 (1 H, d, $J = 9.0$ Hz), 7.91 (1 H, s), 7.08 (1 H, dd, $J = 4.2$ and 9.0 Hz), 3.35–3.10 (5 H, m), 2.31–2.24 (1 H, m), 2.09–2.05 (1 H, m). LC-MS: m/z $[\text{M} + \text{H}]^+$ 213.1192.

***N*-(3-(Trifluoromethyl)-4-((4-methylpiperazin-1-yl)methyl)phenyl)-3-(2-(imidazo[1,2-*b*]pyridazin-3-yl)ethynyl)pyrrolidine-1-carboxamide (1b).** In a similar manner to **1a**, compound **1b** was prepared from **9b** and **10** (46 mg, pale yellow solid, 19%). mp: 83–85 °C. $^1\text{H NMR}$ (300 MHz, CDCl_3): δ 8.44 (1 H, s), 7.98–7.92 (2 H, m), 7.64–7.58 (3 H, m), 7.10 (1 H, dd, $J = 4.5$ and 9.0 Hz), 6.37 (1 H, s), 3.93–3.88 (1 H, m), 3.76 (1 H, m), 3.70–3.49 (4 H, m), 2.62 (8 H, brs), 2.44 (4 H, brs), 2.31–2.29 (2 H, m). HR-MS (ESI-TOF $^+$): m/z $[\text{M} + \text{H}]^+$ calcd for $\text{C}_{26}\text{H}_{29}\text{F}_3\text{N}_7\text{O}$ 512.2380, found 512.2375.

Synthesis of Compounds 2a–k. (3,4-Dinitrophenyl)-(4-methylpiperazin-1-yl)-methanone (12). A mixture of 3,4-dinitrobenzoic acid **11** (10.6 g, 50 mmol) and SOCl_2 (50 mL) was heated at reflux for 6 h. Then, the mixture was evaporated to dryness *in vacuo*. The residue was dissolved in CH_2Cl_2 (50 mL) and cooled to 5 °C. To this solution were added *N*-methylpiperazine (5.5 g, 55 mmol) and Et_3N (5.5 g, 55 mmol) dropwise as a solution in CH_2Cl_2 (50 mL). After stirring overnight at rt, the combined organic phase was washed with water (100 mL), dried over Na_2SO_4 , filtered, and concentrated. The resulting residue was purified by silica gel chromatography (eluent of 5% MeOH in CH_2Cl_2) to give a yellow solid (14.0 g, 95%). $^1\text{H NMR}$ (300 MHz, $\text{DMSO}-d_6$): δ 8.29 (1 H, s), 8.26 (1 H, d, $J = 9.0$ Hz), 7.96 (1 H, d, $J = 9.0$ Hz), 3.62 (2 H, brs), 3.28 (2 H, brs), 2.38 (2 H, brs), 2.26 (2 H, brs), 2.19 (3 H, s).

1-(3,4-Dinitrobenzyl)-4-methylpiperazine (13). To a cooled solution (5 °C) of compound **12** (5.88 g, 20 mmol) in THF was added powdered NaBH_4 (1.89 g, 50 mmol), followed by the dropwise addition of $\text{BF}_3 \cdot \text{Et}_2\text{O}$ (6.4 mL, 50 mmol) while keeping the temperature below 5 °C. The mixture was allowed to come to rt over 2 h and then stirred for a further 3 h at rt. MeOH was then added cautiously to the mixture. Stirring was continued for 10 min, then the mixture was concentrated. The residue was partitioned between EtOAc (150 mL) and saturated aqueous NaHCO_3 (150 mL). The organic layer was washed with water (100 mL) and brine (100 mL), then dried over Na_2SO_4 , filtered, and concentrated. The residue was purified by silica gel chromatography (eluent of 2% MeOH in CH_2Cl_2) to give a yellow solid (4.5 g, 80%). $^1\text{H NMR}$ (400 MHz, CDCl_3): δ 7.92–7.90 (2 H, m), 7.70 (1 H, d, $J = 8.4$ Hz), 3.73 (2 H, s), 3.10–3.07 (2 H, m), 2.99–2.94 (2 H, m), 2.81–2.76 (2 H, m), 2.67 (3 H, s), 2.56–2.53 (2 H, m).

1-(3,4-Diaminobenzyl)-4-methylpiperazine (14). Compound **13** (2.8 g, 10 mmol) was dissolved in DMF/MeOH (1:1, 20 mL) and agitated with 10% Pd/C (280 mg) under an atmosphere of H_2 for 12 h. The reaction was monitored by TLC. The mixture was then filtered and evaporated to give a dark solid, which was used immediately without any further purification.

2-(3-Iodo-4-methylphenyl)-6-((4-methylpiperazin-1-yl)methyl)-1H-benzod[*d*]imidazole (16a). A mixture of compound **14** (10 mmol), 3-iodo-4-methylbenzoic acid **15a** (2.6 g, 10 mmol), EDCI (11 mmol), and HOBt (11 mmol) in dry DMF (25 mL) was stirred at ambient temperature for 24 h. The mixture was then evaporated *in vacuo*, and the crude residue was dissolved in CH_2Cl_2 (100 mL), washed with water (100 mL) and brine (100 mL), dried over Na_2SO_4 , filtered, and concentrated. The residue obtained was dissolved in AcOH (30 mL), and the mixture was heated at reflux for 3 h. The reaction mixture was evaporated *in vacuo*, and the residue was purified by silica gel chromatography (eluent of 10% MeOH in CH_2Cl_2 , MeOH was added to 0.5% Et_3N) to give a yellow solid (1.35 g, 30%). $^1\text{H NMR}$ (300 MHz, CDCl_3): δ 8.50 (1 H, s), 7.96 (1 H, d, $J = 9.0$ Hz), 7.55 (1 H, d, $J = 9.0$ Hz), 7.54 (1 H, d, $J = 9.0$ Hz), 7.30 (1 H, s), 7.22 (1 H, d, $J = 9.0$ Hz), 3.60 (2 H, s), 2.54 (8 H, brs), 2.45 (3 H, s), 2.32 (3 H, s).

2-(4-Chloro-3-iodophenyl)-6-((4-methylpiperazin-1-yl)methyl)-1H-benzod[*d*]imidazole (16b). In a similar manner to **16a**, compound **16b** was prepared from **14** and **15b** (0.9 g, a pale yellow solid, 43%). $^1\text{H NMR}$ (300 MHz, CDCl_3): δ 8.52 (1 H, s), 7.97 (1 H, d, $J = 8.1$ Hz), 7.46–7.36 (2 H, m), 7.24–7.21 (2 H, m), 3.59 (2 H, s), 2.51 (8 H, brs), 2.29 (3 H, s).

3-(2-(2-Methyl-5-(6-((4-methylpiperazin-1-yl)methyl)-1H-benzod[*d*]imidazol-2-yl)phenyl)ethynyl)imidazo[1,2-*b*]pyridazine (2a). Compound **17a** (29 mg, 0.2 mmol), compound **16a** (110 mg, 0.2 mmol), $\text{Pd}(\text{PPh}_3)_4$ (17 mg, 0.015 mmol), and CuI (2 mg, 0.01 mmol) were placed in a two-neck flask with a rubber plug. The mixture underwent three cycles of vacuuming and filling with Ar_2 . Then, a solution of DIPEA (58 mg, 0.45 mmol) and DMF (2 mL) was injected into the flask. The mixture was stirred at rt for 20 h, then poured into 25 mL of water and extracted with CH_2Cl_2 (20 mL \times 3). The organic layer was washed with brine, dried over Na_2SO_4 , and filtered, and the filtrate was evaporated *in vacuo*. The residue was purified by chromatography on silica gel ($\text{CH}_2\text{Cl}_2/\text{CH}_3\text{OH} = 97:3$ to $97:6$) to give 0.1 g of the crude product, and continued purification via preparation TLC ($\text{CH}_2\text{Cl}_2/\text{CH}_3\text{OH} = 120:8$) gave 15 mg of the product as a pale yellow solid (16%). mp: 114–115 °C. $^1\text{H NMR}$ (300 MHz, CDCl_3): δ 8.47 (1 H, d, $J = 3.6$ Hz), 8.25 (1 H, s), 8.15 (1 H, s), 8.11 (1 H, d, $J = 7.5$ Hz), 7.98 (1 H, d, $J = 9.0$ Hz), 7.59 (2 H, brs), 7.36 (1 H, d, $J = 7.8$ Hz), 7.22 (1 H, s), 7.13 (1 H, dd, $J = 9.3$ and 4.2 Hz), 3.64 (2 H, s), 2.60 (11 H, brs), 2.34 (3 H, s). $^{13}\text{C NMR}$ (150 MHz, $\text{DMSO}-d_6$): δ 151.01, 145.53, 141.52, 140.12, 138.71, 131.00, 129.26, 128.71, 127.38, 126.89, 126.59, 124.55, 122.75, 119.53, 119.39, 118.93, 112.25, 110.38, 97.04, 81.40, 62.31, 54.19, 51.51, 44.69, 20.74. HR-MS (ESI-TOF $^+$): m/z $[\text{M} + \text{H}]^+$ calcd for $\text{C}_{28}\text{H}_{28}\text{N}_7$ 462.2401, found 462.2413.

***N*-Cyclobutyl-6-(2-(2-methyl-5-(6-((4-methylpiperazin-1-yl)methyl)-1H-benzod[*d*]imidazol-2-yl)phenyl)ethynyl)pyridazin-3-amine (2b).** In a similar manner to **2a**, compound **2b** was prepared from **16a** and **17b** (87 mg, a pale yellow solid, 59%). mp: 148–150 °C. $^1\text{H NMR}$ (300 MHz, CDCl_3): δ 8.08 (1 H, d, $J = 8.1$ Hz), 7.90 (1 H, s), 7.66–7.63 (2 H, m), 7.24–7.15 (3 H, m), 6.62 (1 H, d, $J = 9.0$ Hz), 5.63 (1 H, d, $J = 6.6$ Hz), 4.33–4.26 (1 H, m), 3.62 (2 H, s), 2.58–2.45 (10 H, m), 2.35 (3 H, s), 2.31 (3 H, s), 2.03–1.94 (2 H, m), 1.85–1.82 (2 H, m). $^{13}\text{C NMR}$ (150 MHz, CDCl_3): δ 157.13, 151.77, 143.32, 142.12, 138.96, 136.96, 131.22, 130.22, 130.12, 129.99, 127.93, 127.54, 126.47, 124.20, 122.43, 112.20, 101.35, 90.23, 89.89, 63.00, 54.63, 52.08, 47.12, 45.38, 31.01, 20.51, 15.29. HR-MS (ESI-TOF $^+$): m/z $[\text{M} + \text{H}]^+$ calcd for $\text{C}_{30}\text{H}_{34}\text{N}_7$ 492.2870, found 492.2856.

***N*-Cyclopropyl-6-(2-(2-methyl-5-(6-((4-methylpiperazin-1-yl)methyl)-1H-benzod[*d*]imidazol-2-yl)phenyl)ethynyl)pyridazin-3-amine (2c).** In a similar manner to **2a**, compound **2c** was prepared from **16a** and **17c** (30 mg, a khaki solid, 28%). mp: 145–146 °C. $^1\text{H NMR}$ (300 MHz, CDCl_3): δ 8.07 (1 H, d, $J = 8.7$ Hz), 7.99 (1 H, s), 7.64–7.61 (2 H, m), 7.39 (1 H, d, $J = 9.3$ Hz), 7.22–7.18 (2 H, m), 7.02 (1 H, d, $J = 9.3$ Hz), 5.98 (1 H, s), 3.61 (2 H, s), 2.55–2.30 (9 H, m), 2.58 (1 H, m), 2.28 (3 H, s), 2.26 (3 H, s), 0.87–0.84 (2 H, m), 0.64 (2 H, brs). $^{13}\text{C NMR}$ (150 MHz, $\text{DMSO}-d_6$): δ 159.65, 150.84, 144.25, 143.45, 141.77, 138.30, 131.14, 130.93, 129.71, 128.73, 127.30, 123.52, 122.77, 119.47, 118.82, 112.31, 111.76, 92.29, 88.42, 62.92, 55.26, 52.99, 46.21, 23.99, 20.70, 7.22. HR-MS (ESI-TOF $^+$): m/z $[\text{M} + \text{H}]^+$ calcd for $\text{C}_{29}\text{H}_{32}\text{N}_7$ 478.2714, found 478.2721.

***N*-Isopropyl-6-(2-(2-methyl-5-(6-((4-methylpiperazin-1-yl)methyl)-1H-benzod[*d*]imidazol-2-yl)phenyl)ethynyl)pyridazin-3-amine (2d).** In a similar manner to **2a**, compound **2d** was prepared from **16a** and **17d** (40 mg, a pale yellow solid, 37%). mp: 129–130 °C. $^1\text{H NMR}$ (300 MHz, CDCl_3): δ 8.07 (1 H, d, $J = 8.1$ Hz), 7.87 (1 H, s), 7.65 (2 H, brs), 7.27 (1 H, s), 7.25–7.19 (2 H, m), 6.62 (1 H, d, $J = 9.0$ Hz), 5.02 (1 H, d, $J = 7.5$ Hz), 4.15–4.11 (1 H, m), 3.61 (2 H, s), 2.43 (8 H, brs), 2.32 (3 H, s), 2.27 (3 H, s), 1.28 (6 H, d, $J = 6.0$ Hz). $^{13}\text{C NMR}$ (150 MHz, CDCl_3): δ 157.13, 151.63, 142.08, 138.83, 131.05, 130.10, 130.08, 129.76, 128.88, 128.36, 127.94, 127.44, 124.14, 122.45, 121.09, 112.68, 90.25, 89.77, 63.38, 55.07, 52.95, 45.94, 43.38, 22.76, 20.50. HR-MS (ESI-TOF $^+$): m/z $[\text{M} + \text{H}]^+$ calcd for $\text{C}_{29}\text{H}_{34}\text{N}_7$ 480.2870, found 480.2847.

N-Cyclopropyl-5-(2-(2-methyl-5-(6-((4-methylpiperazin-1-yl)-methyl)-1*H*-benzo[d]imidazol-2-yl)phenyl)ethynyl)pyrimidin-2-amine (**2e**). In a similar manner to **2a**, compound **2e** was prepared from **16a** and **17e** (30 mg, a brown solid, 23%). mp: 136–137 °C. ¹H NMR (300 MHz, CDCl₃): δ 8.40 (2 H, s), 8.21 (1 H, s), 7.98 (1 H, d, *J* = 8.1 Hz), 7.55–7.48 (2 H, m), 7.23–7.15 (2 H, m), 5.81 (1 H, s), 5.28 (1 H, s), 3.57 (2 H, s), 2.79–2.77 (1 H, m), 2.55 (8 H, brs), 2.46 (3 H, s), 2.32 (3 H, s), 0.87–0.83 (2 H, m), 0.56 (2 H, brs). ¹³C NMR (150 MHz, CDCl₃): δ 161.58, 160.20, 151.64, 141.87, 131.17, 130.90, 130.29, 129.87, 128.89, 128.81, 127.61, 126.43, 125.04, 124.32, 123.69, 108.36, 90.78, 88.66, 62.55, 54.04, 51.12, 44.73, 23.99, 20.75, 7.44. HR-MS (ESI-TOF⁺): *m/z* [M + H]⁺ calcd for C₂₉H₃₂N₇ 478.2714, found 478.2718.

4-(4-Methyl-1*H*-imidazol-1-yl)-2-nitroaniline (**19**). A suspension of 4-bromo-2-nitroaniline **18** (4.34 g, 20 mmol), 4-methylimidazole (1.97 g, 24 mmol), K₂CO₃ (3.04 g, 22 mmol), CuI (0.57 g, 3 mmol) and 8-hydroxyquinoline (0.44 g, 3 mmol) in 20 mL of DMSO was stirred at 120 °C in a sealed tube under Ar₂ for 29 h. The mixture was cooled to rt, and 28% aqueous ammonia (10 mL) was added. To the mixture were added H₂O and EtOAc. The aqueous layer was extracted with EtOAc (80 mL × 3), and the organic layers were washed with brine, dried over Na₂SO₄, and filtered. The filtrate was evaporated in a vacuum, and the residue was washed with PE/EtOAc to give 2.47 g of the product as a red solid (57%). ¹H NMR (300 MHz, DMSO-*d*₆): δ 8.06–8.02 (2 H, m), 7.68 (1 H, dd, *J* = 2.7 and 9.0 Hz), 7.56 (2 H, s), 7.36 (1 H, s), 7.15 (1 H, d, *J* = 9.3 Hz), 2.15 (3 H, s). LC-MS: *m/z* [M + H]⁺ 219.0895.

2-Amino-4-(4-methyl-1*H*-imidazol-1-yl)aniline (**20**). Compound **19** (0.22 g, 1 mmol) was suspended in 20 mL of anhydrous methanol. The mixture was hydrogenated with 0.11 g of Raney Ni at 40 psi for 7 h. Then, the Raney Ni was removed by filtration. The filtrate was evaporated to give 0.18 g of the title compound as a yellow solid (96%), which was used immediately without any further purification.

N-(2-Amino-4-(4-methyl-1*H*-imidazol-1-yl)phenyl)-3-iodo-4-methylbenzamide (**21**). A solution of 3-iodo-4-methylbenzoic acid (0.26 g, 1 mmol) in SOCl₂ (5 mL) was refluxed for 2 h and then evaporated in a vacuum to remove the residual SOCl₂. The residue was dissolved in 5 mL of anhydrous THF and added dropwise to a solution of triethylamine (0.12 g, 1.2 mmol), compound **20** (0.18 g, 1 mmol), and DMAP (24 mg) in 5 mL of anhydrous THF. The result mixture was stirred at rt for 20 h and then evaporated in a vacuum. The residue was purified by chromatography on silica gel (CH₂Cl₂/CH₃OH = 97:3) to give 0.16 g of the product as a pale yellow solid (37%). LC-MS: *m/z* [M + H]⁺ 433.0520.

2-(3-Iodo-4-methylphenyl)-6-(4-methyl-1*H*-imidazol-1-yl)-1*H*-benzo[d]imidazole (**22**). A solution of compound **21** (0.16 g, 0.37 mmol) in 5 mL of glacial acetic acid was refluxed for 8 h. Then, the mixture was evaporated in a vacuum, and the residue was purified by chromatography on silica gel (CH₂Cl₂/CH₃OH = 97:3 to 94:6) to give 0.1 g of the product as a pale yellow solid (65%). ¹H NMR (300 MHz, DMSO-*d*₆): δ 8.65 (1 H, s), 8.13–8.11 (2 H, m), 7.71 (1 H, d, *J* = 8.4 Hz), 7.55–7.51 (2 H, m), 7.45–7.39 (3 H, m), 2.45 (3 H, s), 2.19 (3 H, s). LC-MS: *m/z* [M + H]⁺ 415.0409.

3-((2-Methyl-5-(5-(4-methyl-1*H*-imidazol-1-yl)-1*H*-benzo[d]imidazol-2-yl)phenyl)ethynyl)imidazo[1,2-*b*]pyridazine (**2f**). In a similar manner to **2a**, compound **2f** was prepared from **17a** and **22** (80 mg, a pale yellow solid, 63%). mp: 182–184 °C. ¹H NMR (400 MHz, CD₃OD): δ 8.57 (1 H, d, *J* = 3.6 Hz), 8.36 (1 H, s), 8.24 (1 H, s), 8.05–7.98 (3 H, m), 7.70 (1 H, s), 7.67 (1 H, d, *J* = 9.0 Hz), 7.47–7.40 (3 H, m), 7.30 (1 H, dd, *J* = 4.2 and 9.2 Hz), 2.59 (3 H, s), 2.28 (3 H, s). ¹³C NMR (150 MHz, CD₃OD): δ 153.42, 144.66, 142.71, 139.83, 136.69, 134.16, 134.04, 131.52, 130.27, 129.41, 126.93, 126.81, 124.99, 123.15, 119.10, 117.19, 116.93, 112.97, 96.26, 80.08, 19.47, 9.94. HR-MS (ESI-TOF⁺): *m/z* [M + H]⁺ calcd for C₂₆H₂₀N₇ 430.1775, found 430.1778.

3-(2-(2-Chloro-5-(6-((4-methylpiperazin-1-yl)methyl)-1*H*-benzo[d]imidazol-2-yl)phenyl)ethynyl)imidazo[1,2-*b*]pyridazine (**2g**). In a similar manner to **2a**, compound **2g** was prepared from **17a** and **16b** (80 mg, a khaki solid, 78%). mp: 156–157 °C. ¹H NMR (300 MHz, CDCl₃): δ 8.43 (1 H, s), 8.36 (1 H, s), 8.14–8.11 (2 H, m), 7.93 (1

H, d, *J* = 9.3 Hz), 7.54–7.46 (3 H, m), 7.19 (1 H, d, *J* = 7.8 Hz), 7.11 (1 H, d, *J* = 4.5 Hz), 3.60 (2 H, s), 2.61 (8 H, brs), 2.31 (3 H, s). ¹³C NMR (150 MHz, CDCl₃): δ 150.51, 144.10, 139.92, 139.86, 138.81, 138.72, 137.06, 131.16, 130.45, 130.11, 128.93, 128.07, 125.76, 123.17, 123.11, 118.25, 118.09, 117.68, 112.90, 94.94, 81.51, 62.76, 54.36, 51.64, 45.08. HR-MS (ESI-TOF⁺): *m/z* [M + H]⁺ calcd for C₂₇H₂₅ClN₇ 482.1854, found 482.1841.

6-(2-(2-Chloro-5-(6-((4-methylpiperazin-1-yl)methyl)-1*H*-benzo[d]imidazol-2-yl)phenyl)ethynyl)-*N*-cyclobutylpyridazin-3-amine (**2h**). In a similar manner to **2a**, compound **2g** was prepared from **17b** and **16b** (70 mg, a pale yellow solid, 64%). mp: 161–163 °C. ¹H NMR (300 MHz, CDCl₃): δ 8.14 (1 H, d, *J* = 7.2 Hz), 7.95 (1 H, s), 7.65–7.62 (2 H, m), 7.38 (1 H, d, *J* = 8.7 Hz), 7.31 (1 H, d, *J* = 9.0 Hz), 7.19 (1 H, d, *J* = 8.1 Hz), 6.65 (1 H, d, *J* = 9.3 Hz), 5.80 (1 H, d, *J* = 5.7 Hz), 4.30–4.28 (1 H, m), 3.63 (2 H, s), 2.63–2.40 (13 H, m), 2.02–1.96 (2 H, m), 1.81–1.79 (2 H, m). ¹³C NMR (100 MHz, CDCl₃): δ 157.22, 150.53, 138.33, 136.91, 132.49, 131.47, 131.26, 130.01, 129.87, 129.56, 129.19, 129.06, 128.51, 128.02, 124.56, 122.41, 112.27, 91.11, 87.86, 63.23, 54.85, 52.63, 47.08, 45.73, 30.94, 15.29. HR-MS (ESI-TOF⁺): *m/z* [M + H]⁺ calcd for C₂₉H₃₁ClN₇ 512.2324, found 512.2303.

6-(2-(2-Chloro-5-(6-((4-methylpiperazin-1-yl)methyl)-1*H*-benzo[d]imidazol-2-yl)phenyl)ethynyl)-*N*-cyclopropylpyridazin-3-amine (**2i**). In a similar manner to **2a**, compound **2i** was prepared from **17c** and **16b** (30 mg, a khaki solid, 28%). mp: 130–131 °C. ¹H NMR (300 MHz, CDCl₃): δ 8.12 (1 H, d, *J* = 8.1 Hz), 7.86 (1 H, s), 7.64–7.55 (2 H, m), 7.45–7.39 (2 H, m), 7.22 (1 H, s), 7.02 (1 H, d, *J* = 9.3 Hz), 6.00 (1 H, s), 3.61 (2 H, s), 2.60–2.44 (9 H, m), 2.27 (3 H, s), 0.89–0.87 (2 H, m), 0.65 (2 H, brs). ¹³C NMR (150 MHz, DMSO-*d*₆): δ 159.75, 149.77, 144.31, 143.38, 137.73, 135.89, 131.25, 130.68, 130.01, 128.60, 124.79, 123.74, 122.66, 119.60, 119.01, 112.18, 111.55, 93.32, 86.35, 62.88, 55.24, 52.98, 46.19, 23.99, 7.20. HR-MS (ESI-TOF⁺): *m/z* [M + H]⁺ calcd for C₂₈H₂₉ClN₇ 498.2167, found 498.2150.

6-(2-(2-Chloro-5-(6-((4-methylpiperazin-1-yl)methyl)-1*H*-benzo[d]imidazol-2-yl)phenyl)ethynyl)-*N*-isopropylpyridazin-3-amine (**2j**). In a similar manner to **2a**, compound **2j** was prepared from **17d** and **16b** (70 mg, a khaki solid, 65%). mp: 127–128 °C. ¹H NMR (300 MHz, CDCl₃): δ 8.12 (1 H, d, *J* = 7.5 Hz), 7.82 (1 H, s), 7.64–7.53 (3 H, m), 7.36 (1 H, d, *J* = 8.4 Hz), 7.30 (1 H, d, *J* = 9.3 Hz), 6.68 (1 H, d, *J* = 9.3 Hz), 5.22 (1 H, d, *J* = 6.6 Hz), 4.14–4.12 (1 H, m), 3.62 (2 H, s), 2.51 (8 H, brs), 2.31 (3 H, s), 1.30 (6 H, d, *J* = 6.0 Hz). ¹³C NMR (100 MHz, CDCl₃): δ 162.61, 157.33, 150.63, 138.26, 136.97, 131.33, 131.24, 129.82, 129.58, 129.23, 129.15, 128.56, 128.03, 124.53, 123.48, 122.37, 112.98, 91.14, 87.85, 63.31, 55.03, 52.84, 45.89, 43.45, 22.73. HR-MS (ESI-TOF⁺): *m/z* [M + H]⁺ calcd for C₂₈H₃₁ClN₇ 500.2324, found 500.2313.

5-(2-(2-Chloro-5-(6-((4-methylpiperazin-1-yl)methyl)-1*H*-benzo[d]imidazol-2-yl)phenyl)ethynyl)-*N*-cyclopropylpyrimidin-2-amine (**2k**). In a similar manner to **2a**, compound **2k** was prepared from **17e** and **16b** (10 mg, a brown solid, 9%). mp: 160–162 °C. ¹H NMR (300 MHz, CDCl₃): δ 8.44 (2 H, d, *J* = 4.5 Hz), 8.13 (1 H, d, *J* = 7.8 Hz), 7.59 (1 H, d, *J* = 7.5 Hz), 7.52 (1 H, s), 7.46 (1 H, d, *J* = 8.7 Hz), 7.39 (1 H, d, *J* = 8.4 Hz), 7.16 (1 H, d, *J* = 7.5 Hz), 5.80 (1 H, s), 3.60 (2 H, s), 3.12–2.81 (9 H, m), 2.59 (3 H, s), 0.88–0.82 (2 H, m), 0.61–0.58 (2 H, m). ¹³C NMR (150 MHz, DMSO-*d*₆): δ 162.27, 160.69, 150.22, 135.87, 135.60, 134.96, 130.98, 130.71, 130.56, 129.84, 129.50, 128.87, 128.69, 128.11, 123.31, 105.93, 91.36, 88.80, 63.27, 52.90, 49.61, 45.79, 24.41, 6.78. HR-MS (ESI-TOF⁺): *m/z* [M + H]⁺ calcd for C₂₈H₂₉ClN₇ 498.2167, found 498.2163.

Synthesis of Compounds 3a–e. 3,3-Difluoro-1-(4-methylpiperazin-1-yl)-2,3-dihydro-1*H*-inden-5-amine (**24**). Compound **23** (0.15 g, 0.5 mmol) was dissolved in MeOH (20 mL) and agitated with 10% Pd/C (15 mg) under an atmosphere of H₂ for 12 h. The reaction was monitored by TLC. The mixture was then filtered and evaporated to give a gray solid, which was used immediately without any further purification.

N-(3,3-Difluoro-1-(4-methylpiperazin-1-yl)-2,3-dihydro-1*H*-inden-5-yl)-3-iodo-4-methylbenzamide (**25a**). 3-Iodo-4-methylbenzoyl chloride, which was prepared from the reaction of 3-iodo-4-methylbenzoic acid (79 mg, 0.3 mmol) and SOCl₂, was added to a

solution of compound **24** (78 mg, 0.3 mmol), Et₃N (37 mg, 0.36 mmol), and a catalytic amount of DMAP in THF (5 mL). After stirring at rt overnight, the reaction was quenched with water, extracted with CH₂Cl₂ (20 mL × 3), dried over Na₂SO₄, and purified by chromatography on silica gel (CH₂Cl₂/MeOH = 95:5) to afford 140 mg of the product as a yellow solid in a 92% yield. LC-MS: *m/z* [M + H]⁺ 512.1049.

N-(3,3-Difluoro-1-(4-methylpiperazin-1-yl)-2,3-dihydro-1*H*-inden-5-yl)-3-iodobenzamide (**25b**). In a similar manner to **25a**, compound **25b** was prepared from compound **24** and 3-iodo-benzoyl chloride (100 mg, yellow solid, 51%). LC-MS: *m/z* [M + H]⁺ 498.0801.

N-(3,3-Difluoro-1-(4-methylpiperazin-1-yl)-2,3-dihydro-1*H*-inden-5-yl)-3-(imidazo[1,2-*b*]pyridazin-3-ylethynyl)-4-methylbenzamide (**3a**). Compound **17a** (27 mg, 0.19 mmol), compound **25a** (80 mg, 0.16 mmol), Pd(PPh₃)₄ (9 mg, 0.008 mmol), and CuI (2.2 mg, 0.012 mmol) were placed in a two-neck flask with a rubber plug. The mixture underwent three cycles of vacuuming and filling with Ar₂, then a solution of DIPEA (30 mg, 0.24 mmol) and DMF (2 mL) was injected into the flask. The mixture was stirred at rt for 20 h and then poured into 25 mL of water and extracted with CH₂Cl₂ (20 mL × 3). The organic layer was washed with brine, dried with Na₂SO₄, and filtered, and the filtrate was evaporated in a vacuum. The residue was purified by chromatography on silica gel (CH₂Cl₂/CH₃OH = 97:3 to 97:6) to give 50 mg of the crude product, and continued purification via preparation TLC (CH₂Cl₂/CH₃OH = 150:15) gave 25 mg of the product as a pale yellow solid (30%). mp: 111–113 °C. ¹H NMR (300 MHz, CDCl₃): δ 8.48 (1 H, d, *J* = 4.2 Hz), 8.18 (1 H, s), 8.08 (1 H, s), 8.06 (1 H, d, *J* = 1.8 Hz), 7.98 (1 H, dd, *J* = 9.6 and 1.5 Hz), 7.88–7.80 (3 H, m), 7.48 (1 H, d, *J* = 8.7 Hz), 7.39 (1 H, d, *J* = 8.7 Hz), 7.13 (1 H, dd, *J* = 9.0 and 4.2 Hz), 4.52–4.50 (1 H, m), 2.67–2.58 (7 H, m), 2.49 (6 H, brs), 2.31 (3 H, s). ¹³C NMR (150 MHz, CDCl₃): δ 164.90, 144.54, 143.95, 139.77, 139.51, 138.76, 138.40, 137.91 (t, *J* = 26.0 Hz), 132.29, 130.26, 130.05, 127.94 (t, *J* = 24.1 Hz), 127.82, 126.35, 125.94, 124.02, 122.91, 117.82, 114.28, 113.10, 96.65, 80.83, 64.35, 55.21, 45.86, 35.34 (t, *J* = 23.3 Hz), 20.95. HR-MS (ESI-TOF⁺): *m/z* [M + H]⁺ calcd for C₃₀H₂₉F₂N₆O 527.2365, found 527.2331.

3-((2-(Cyclopropylamino)pyrimidin-5-yl)ethynyl)-*N*-(3,3-difluoro-1-(4-methylpiperazin-1-yl)-2,3-dihydro-1*H*-inden-5-yl)-4-methylbenzamide (**3b**). In a similar manner to **3a**, compound **3b** was prepared from **17e** and **25a** (10 mg, a pale yellow solid, 23%). mp: 95–97 °C. ¹H NMR (300 MHz, CDCl₃): δ 8.50 (2 H, s), 7.95 (1 H, s), 7.91 (1 H, s), 7.85 (1 H, d, *J* = 8.1 Hz), 7.79–7.74 (2 H, m), 7.48 (1 H, d, *J* = 7.8 Hz), 7.36 (1 H, d, *J* = 8.1 Hz), 4.51–4.49 (1 H, m), 2.82 (1 H, brs), 2.67–2.47 (13 H, m), 2.30 (3 H, s), 0.94–0.85 (2 H, m), 0.62–0.60 (2 H, m). ¹³C NMR (150 MHz, CDCl₃): δ 164.86, 161.63, 160.24, 144.15, 139.42, 138.65, 137.90 (t, *J* = 26.1 Hz), 132.20, 130.15, 130.03, 127.87 (t, *J* = 243.3 Hz), 127.02, 126.31, 123.98, 123.55, 114.23, 108.11, 90.40, 89.14, 64.33, 55.12, 45.71, 35.53 (t, *J* = 23.0 Hz), 29.70, 23.98, 20.89, 7.43. HR-MS (ESI-TOF⁺): *m/z* [M + H]⁺ calcd for C₃₁H₃₃F₂N₆O 543.2684, found 543.2654.

N-(3,3-Difluoro-1-(4-methylpiperazin-1-yl)-2,3-dihydro-1*H*-inden-5-yl)-3-(imidazo[1,2-*b*]pyridazin-3-ylethynyl)benzamide (**3c**). In a similar manner to **3a**, compound **3c** was prepared from **17a** and **25b** (15 mg, a pale yellow solid, 29%). mp: 136–138 °C. ¹H NMR (400 MHz, CDCl₃): δ 8.49 (1 H, d, *J* = 3.2 Hz), 8.19 (1 H, s), 8.09 (2 H, s), 7.98 (1 H, d, *J* = 9.2 Hz), 7.92–7.85 (3 H, m), 7.78 (1 H, d, *J* = 7.6 Hz), 7.54–7.48 (2 H, m), 7.13 (1 H, dd, *J* = 9.2 and 4.0 Hz), 4.52–4.50 (1 H, m), 2.67–2.48 (10 H, m), 2.31 (3 H, s). ¹³C NMR (150 MHz, CDCl₃): δ 164.81, 143.95, 140.76, 139.76, 139.53, 138.78, 138.58, 137.98 (t, *J* = 25.9 Hz), 135.00, 129.81, 129.17, 127.89 (t, *J* = 249.2 Hz), 127.68, 126.37, 126.02, 124.01, 123.27, 117.85, 114.31, 112.88, 97.57, 64.34, 55.11, 45.69, 35.55 (t, *J* = 23.1 Hz), 29.70. HR-MS (ESI-TOF⁺): *m/z* [M + H]⁺ calcd for C₂₉H₂₇F₂N₆O 513.2209, found 513.2200.

3-((2-(Cyclopropylamino)pyrimidin-5-yl)ethynyl)-*N*-(3,3-difluoro-1-(4-methylpiperazin-1-yl)-2,3-dihydro-1*H*-inden-5-yl)-benzamide (**3d**). In a similar manner to **3a**, compound **3d** was prepared from **17e** and **25b** (10 mg, a pale yellow solid, 19%). mp: 105–107 °C. ¹H NMR (400 MHz, CDCl₃): δ 8.50 (1 H, s), 7.98 (1

H, s), 7.95 (1 H, s), 7.85 (2 H, d, *J* = 8.0 Hz), 7.80 (1 H, s), 7.68 (1 H, d, *J* = 7.6 Hz), 7.52–7.47 (2 H, m), 5.55 (1 H, s), 4.51–4.49 (1 H, m), 2.82 (1 H, m), 2.66–2.52 (10 H, m), 2.36 (3 H, s), 0.91–0.86 (2 H, m), 0.59 (2 H, brs). ¹³C NMR (150 MHz, CDCl₃): δ 164.90, 161.63, 160.40, 139.30, 138.66, 137.99 (t, *J* = 26.1 Hz), 134.91, 134.62, 129.75, 129.11, 127.77 (t, *J* = 243.0 Hz), 126.96, 126.30, 124.07, 123.93, 114.34, 107.87, 91.41, 85.53, 64.31, 54.96, 45.33, 35.65 (t, *J* = 22.8 Hz), 29.71, 23.98, 7.44. HR-MS (ESI-TOF⁺): *m/z* [M + H]⁺ calcd for C₃₁H₃₄F₂N₆O 529.2522, found 529.2506.

3,3-Difluoro-2-(4-methylpiperazin-1-yl)-2,3-dihydro-1*H*-inden-5-amine (**27**). Compound **26** (1.06 g, 3.56 mmol) was dissolved in MeOH (20 mL) and agitated with 10% Pd/C (15 mg) under an atmosphere of H₂ for 12 h. The reaction was indicated by TLC. The mixture was then filtered and evaporated to give a gray solid, which was used immediately without any further purification.

N-(3,3-Difluoro-2-(4-methylpiperazin-1-yl)-2,3-dihydro-1*H*-inden-5-yl)-3-iodo-4-methylbenzamide (**28**). In a similar manner to **25a**, compound **28** was prepared from compound **27** and 3-iodo-4-methylbenzoyl chloride (220 mg, a colorless solid, 86%). LC-MS: *m/z* [M + H]⁺ 512.0918.

N-(3,3-Difluoro-2-(4-methylpiperazin-1-yl)-2,3-dihydro-1*H*-inden-5-yl)-3-(imidazo[1,2-*b*]pyridazin-3-ylethynyl)-4-methylbenzamide (**3e**). In a similar manner to **3a**, compound **3e** was prepared from **17a** and **28** (5 mg, a pale yellow solid, 5%). mp: 250–252 °C. ¹H NMR (400 MHz, CDCl₃): δ 8.48 (1 H, d, *J* = 3.2 Hz), 8.08–8.05 (3 H, m), 8.00 (1 H, d, *J* = 9.2 Hz), 7.83–7.78 (3 H, m), 7.40 (1 H, d, *J* = 7.6 Hz), 7.29 (1 H, s), 7.13 (1 H, dd, *J* = 8.8 and 4.0 Hz), 4.50–4.52 (1 H, m), 3.27–2.96 (6 H, m), 2.74–2.64 (7 H, m), 2.36 (3 H, s). ¹³C NMR (150 MHz, CDCl₃): δ 164.78, 144.53, 143.92, 139.77, 138.43, 137.67, 136.58 (t, *J* = 21.5 Hz), 135.65, 132.25, 130.26, 130.03, 127.71, 126.76 (t, *J* = 234.0 Hz), 125.96, 125.91, 124.07, 122.99, 117.78, 114.86, 113.07, 96.65, 80.87, 69.76 (t, *J* = 23.7 Hz), 54.54, 32.54, 29.70. HR-MS (ESI-TOF⁺): *m/z* [M + H]⁺ calcd for C₃₀H₂₉F₂N₆O: 527.2365, found 527.2337.

Separation of the Optical Isomers of Compound 3a. The racemate product **3a** (0.2 g) was subjected to a separation by the SFC method using a chiral column (CHIRALCEL AS-H, 0.46 cm I.D. × 25 cm-L). Mobile phase: CO₂/MeOH (0.1% DEA) = 60/40 (v/v). Flow rate: 2.0 mL/min. Wavelength: UV 254 nm. The products were respectively collected at peak 1 with a retention time of 19.492 min (**3a-P1**, 89 mg, [α]_D²⁰ = +15.96 (c 1.0, CHCl₃)) and peak 2 with a retention time of 24.422 min (**3a-P2**, 90 mg, [α]_D²⁰ = −16.19 (c 1.0, CHCl₃)).

Separation of the Optical Isomers of Compound 3b. The racemate product **3b** (0.16 g) was subjected to separation by the SFC method using a chiral column (CHIRALCEL OJ-H, 0.46 cm I.D. × 25 cm-L). Mobile phase: CO₂/EtOH (0.1% DEA) = 75/25 (v/v). Flow rate: 2.0 mL/min. Wavelength: UV 280 nm. The products were respectively collected at peak 1 with a retention time of 7.093 min (**3b-P1**, 57 mg, [α]_D²⁰ = +14.79 (c 1.0, CHCl₃)) and peak 2 with a retention time of 8.287 min (**3b-P2**, 69 mg, [α]_D²⁰ = −12.69 (c 1.0, CHCl₃)).

Synthesis of Compound 3a-P1. (S)-1-(3,3-Difluoro-5-nitro-2,3-dihydro-1*H*-inden-1-yl)-4-methylpiperazine (**(S)-23**). To a solution of compound **23** (5 g, 16.8 mmol) in 50 mL of methanol was added *D*-camphorsulfonic acid (8.99 g, 38.7 mmol) at room temperature. Then, 100 mL of isopropanol was added. The mixture was refluxed and then cooled to room temperature. The solution was stirred at rt overnight, and the resultant solid was collected by filtration (5 g). The solid was recrystallized in a solution of methanol/isopropanol = 1:3 to give a colorless solid (4.1 g, 32%). The solid was dissolved in 20 mL of H₂O, then a 15 mL of a 1 mol/L NaOH solution was added in dropwise. The mixture was stirred for 0.5 h, then the aqueous layer was separated, which was further extracted with CH₂Cl₂ (3 × 20 mL). The combined organic layers were washed with brine, dried over Na₂SO₄, and evaporated to give 1.6 g of the product as yellow oil (100%). ¹H NMR (400 MHz, CDCl₃): δ 8.47–8.36 (2 H, m), 7.66 (1 H, d, *J* = 8.4 Hz), 4.58 (1 H, brs), 2.74–2.55 (10 H, m), 2.36 (3 H, s). [α]_D²⁰ = +18.51 (c 1.1, CHCl₃).

(*S*)-*N*-(3,3-Difluoro-1-(4-methylpiperazin-1-yl)-2,3-dihydro-1*H*-inden-5-yl)-3-(imidazo[1,2-*b*]pyridazin-3-ylethynyl)-4-methylbenzamide (**3a-P1**). In a similar manner to **3a**, compound **3a-P1** was prepared from compound (*S*)-**23** (25 mg, a pale yellow solid, 37%). mp: 125–127 °C. $[\alpha]_D^{25} = +13.5$ (c 1.0, CHCl₃). ¹H NMR (400 MHz, CDCl₃): δ 8.49 (1 H, d, *J* = 3.6 Hz), 8.08–8.06 (2 H, m), 7.99 (1 H, d, *J* = 9.2 Hz), 7.87 (1 H, d, *J* = 8.4 Hz), 7.83–7.81 (2 H, m), 7.48 (1 H, d, *J* = 8.4 Hz), 7.40 (1 H, d, *J* = 8.0 Hz), 7.15 (1 H, dd, *J* = 8.8 and 4.0 Hz), 4.51 (1 H, brs), 2.65–2.52 (13 H, m), 2.35 (3 H, s). ¹³C NMR (150 MHz, CDCl₃): δ 164.98, 144.48, 143.94, 139.75, 139.55, 138.81, 138.36, 137.87 (t, *J* = 26.3 Hz), 132.31, 130.23, 130.06, 127.97 (t, *J* = 240.8 Hz), 127.91, 126.34, 125.90, 124.05, 122.82, 117.83, 114.31, 113.12, 96.66, 80.77, 64.36, 55.57, 45.97, 35.48 (t, *J* = 21.8 Hz), 20.93. HR-MS (ESI-TOF⁺): *m/z* [M + H]⁺ calcd for C₃₀H₂₉F₂N₆O 527.2365, found 527.2355.

(*S*)-*N*-(3,3-Difluoro-1-(4-methylpiperazin-1-yl)-2,3-dihydro-1*H*-inden-5-yl)-3-(imidazo[1,2-*b*]pyridazin-3-ylethynyl)-4-methylbenzamide Hydrochloride (**3a-P1-HCl**). To a solution of **3a-P1** (3.93 g, 7.5 mmol) in acetone (110 mL) was added 1 M HCl in an EtOH solution (6.7 mL, 6.7 mmol). The mixture was stirred at rt for 6 h and then filtered. The resultant solid was washed with acetone and dried to give the product as a pale yellow solid (3.84 g, 102%). mp: 240–242 °C. ¹H NMR (400 MHz, DMSO-*d*₆): δ 10.99 (1 H, brs), 10.63 (1H, s), 8.71 (1 H, dd, *J* = 4.4 and 1.2 Hz), 8.25 (1 H, dd, *J* = 9.2 and 1.6 Hz), 8.22 (1 H, s), 8.20 (1 H, d, *J* = 1.6 Hz), 8.13 (1 H, s), 8.02 (1 H, d, *J* = 8.4 Hz), 7.97 (1 H, dd, *J* = 8.0 and 1.6 Hz), 7.54 (1 H, d, *J* = 8.4 Hz), 7.46 (1 H, d, *J* = 8.4 Hz), 7.38 (1 H, dd, *J* = 8.8 and 4.4 Hz), 4.63 (1 H, brs), 3.39–3.30 (2 H, m), 3.05–2.95 (3 H, m), 2.77–2.48 (11 H, m). ¹³C NMR (100 MHz, DMSO-*d*₆): δ 164.59, 145.03, 143.39, 140.21, 139.61, 138.18, 136.68 (*J* = 26.3 Hz), 132.29, 130.22, 129.99, 128.50, 128.43 (*J* = 239.7 Hz), 126.06, 125.97, 124.36, 121.73, 119.05, 113.65, 111.68, 96.40, 81.08, 63.18, 52.57, 46.45, 42.75, 41.88, 35.44 (*J* = 24.4 Hz), 20.36. HR-MS (ESI-TOF⁺): *m/z* [M-HCl+H]⁺ calcd for C₃₀H₂₉F₂N₆O 527.2365, found 527.2361.

Cell Lines and Reagents. The cell lines K562, Ku812, U937, and JURKAT were obtained from the American Type Culture Collection (ATCC) (Manassas, VA). Native or T3151-mutated BCR-ABL cDNAs were cloned into the expression lentiviral vector pCDH-CMV-MCS-EF1-Puro (System Biosciences, Mountain View, CA). Recombinant lentivirus was produced in 293TN cells with lentiviral vectors and packaging plasmids using lipofectamine 2000 (Thermo Fisher Scientific, Waltham, MA). Two days after the lentiviral infection, the stably transduced BaF3 cells were established by selection with 2 μg/mL puromycin for 2 weeks. All the cells were cultured in RPMI 1640 supplemented with 10% FBS (Atlanta Biological, Atlanta, GA) and 1% penicillin/streptomycin (Thermo Fisher Scientific).

Cell Cytotoxicity Assays. K562 and BaF3 (BCR-ABL^{T3151}) cells were cultured in RPMI 1640 with 10% FBS and 100 units/mL penicillin/streptomycin. The cell cytotoxicity assay was performed with the trypan blue assay. K562 and BaF3 (BCR-ABL^{T3151}) cells were seeded in 24-well plates with 1.5 × 10⁵ cells/mL per well, then the cells were treated with ponatinib and test compounds dosed as 100 nM for 48 h. Then, the cells were harvested at 4000 rpm × 4 min and resuspended in 150 μL of PBS. A total of 10 μL of the resuspended cells was stained with an equal volume of a 0.4% trypan blue solution. The stained cell samples were added to the slide, and the number of positive and negative trypan blue cells was counted by an automatic cell counter TC20 (Bio-Rad, Richmond, CA).

Cell Proliferation Assays. Cells were seeded in 24-well plates (0.5 × 10⁵ cells/well) and incubated with increasing concentrations of BCR-ABL inhibitors for 72 h. The inhibitor concentrations tested ranged from 0 to 200 nM for cells expressing BCR-ABL and 0 to 10 000 nM for BCR-ABL-negative cells. Proliferation was assessed using the Vybrant MTT cell proliferation assay kit (Thermo Fisher Scientific).

Western Blot Analysis. A total of 1 × 10⁶ cells were treated in 6-well plates for 6 h with the indicated compounds. Cell lysates were prepared in a RIPA buffer supplemented with a protease/phosphatase inhibitor cocktail (Roche Diagnostics, Indianapolis, IN) and subjected

to SDS-PAGE, followed by a transfer to the PVDF membranes (BioRad, Hercules, CA). Membranes were immunoblotted with the antibodies against phospho-c-ABL (Y245), phospho-CrkI (Y207), and eIF 4E, which were purchased from Cell Signaling Technology (Danvers, MA). Binding was detected with the Pierce ECL Western blotting substrate (Thermo Scientific).

Pharmacokinetic Studies. An animal care and use application for the study was approved by the Institutional Animal Care and Use Committee of Shanghai Institute of Materia Medica, Chinese Academy of Sciences. The tested compounds were subjected to PK in ICR mice (male) weighing 20 to 25 g, with four mice in the oral administration group and three mice in the intravenous injection group. The tested compounds were formulated at a concentration of 10 mg/mL for a 15 mg/kg dose given orally and at a concentration of 1 mg/mL for a 5 mg/kg dose given intravenously. The tested compound was formulated in a 25 mM sodium citrate buffer (pH 2.75) for p.o. administration and with 5% DMSO/5% Tween 80/90% physiological saline for i.v. administration. Blood samples were collected at 0.25, 0.5, 1, 2, 3, 5, 7, 9, and 24 h after oral dosing and 5 min and 0.25, 0.5, 1, 2, 3, 5, 7, 9, and 24 h after i.v. administration. Plasma was harvested and stored at –20 °C until analyzed. Plasma samples were extracted with acetonitrile that contained propranolol as an internal standard using a 3:1 extractant-to-plasma ratio. The concentrations of the tested compound were determined by high-pressure liquid chromatography/tandem mass spectrometry (LC/MS/MS). Chromatographic separation was performed on a Zorbax SB-C18 column (100 mm × 2.1 mm, 3.5 μm) with an isocratic mobile phase of acetonitrile/water (70:30, v/v) containing 0.1% formic acid at a flow rate of 0.2 mL/min. The oral bioavailability was calculated as the ratio between the area under the curve (AUC) following the intravenous administration corrected for the dose ($F = (AUC_{p.o.} \times \text{dose}_{i.v.}) / (AUC_{i.v.} \times \text{dose}_{p.o.}) \times 100\%$).

Mice Xenograft Tumor Models. The experimental protocols were approved by the Institutional Animal Care and Use Committee of Shaanxi Normal University. Fifty female BALB/c-nu mice (SPF (Beijing) Biotechnology Co., Ltd., Beijing, China) were implanted subcutaneously in the right flank with 5 × 10⁶ cells of BaF3/BCR-ABL^{T3151} cells. Tumor volumes were measured using a digital caliper and calculated using the following formula: $V = 0.5 \times \text{width}^2 \times \text{length}$, where *V* stands for tumor volume. When the tumor sizes approached 100–150 mm³, the mice were divided randomly into groups to be treated once daily by oral gavage with either the vehicle or the BCR-ABL inhibitor (10 mice per group). When the dosing period was finished, the TGI was determined with the formula: $TGI = \{1 - [(V_{te} - V_{to}) / (V_{ce} - V_{co})]\} \times 100\%$, where *V*_{te} is the mean tumor volume of the treated group at the final measurement, *V*_{to} is the mean tumor volume of the treated group at the first measurement, *V*_{ce} is the mean tumor volume of control group at the final measurement, and *V*_{co} is the mean tumor volume of control group at the first measurement.

Inhibition Evaluation of the hERG K⁺ Channel. HEK293 cells were stably transfected with the human ether-a-go-go-related gene (hERG) channel. The voltage-gated hERG potassium channel current was recorded at room temperature (25 °C) from randomly selected transfected cells using a whole-cell manual patch clamp system equipped with a EPC10 USB (HEKA) or Multiclamp 700B amplifier (Molecular Devices), while electrical data were digitalized by a Digidata1440A system with a sampling frequency at 10 kHz using a Patchmaster instrument or pClamp10, respectively. The hERG current inhibition was tested in the presence of five concentrations of the inhibitor (30, 10, 3.0, 1.0, and 0.3 μM) for the IC₅₀ determination. Dofetilide was also included as a positive control to ensure the accuracy and sensitivity of the test system. All experiments were performed in duplicate for the IC₅₀ determination.

Ames Assay. Five strains of *Salmonella typhimurium* bacteria (TA97a, TA98, TA100, TA102, and TA1535) were used in the study, which were originally obtained from Bioplus Biotech (Shanghai, CN). DMSO was used as the solvent and the vehicle control, and the highest concentration tested was 312.5 μg/plate. Bacteria, the tested compound, or the vehicle or positive control formulation and a 10% S9 mixture or PBS buffer were added to molten agar at 37 °C, mixed

rapidly, and poured onto a 6-well plate containing minimal agar medium. After the agar was solidified, the plates were inverted and incubated at 37 °C for 48–72 h. Revertant colonies were counted manually, and the background lawn was inspected for signs of cytotoxicity. The results were considered to be positive for mutagenic potential if the increase in the mean revertants at the peak of the dose–response was greater than two- or threefold of the mean solvent or vehicle control value and the increase was dose related.

Chromosome Aberration Test. Chinese hamster lung fibroblasts were used in the test. Cells were treated with a 0.25% EDTA-trypsin solution to prepare the cell suspension (5.0×10^5 cells/mL) and cultured for 24 h in a humidified atmosphere of 5% CO₂ in air at 37 °C. Cultures treated with the metabolic activation system were re-fed with the serum-free S9 mix just before treatment. Compounds were dissolved in DMSO and added to the cultures, and the cultures were incubated at 37 °C. Treatments were for either 4 or 20 h, and aberrations were scored in cells harvested 20 h after the beginning of the treatment. At the termination, the cultures were washed twice with Hank's balanced salt solution and re-fed with the culture medium. Cultures were incubated for a further 18–20 h. Colcemid (0.1 mL) was added 4 h before the monolayers were harvested by trypsinization. A cell sample was counted using a Coulter counter to determine the cell number as an indicator of the cytotoxicity. The viable cells were verified by checking samples for trypan blue dye exclusion. The cells were treated with hypotonic KCl (75 mM) for 25 min at room temperature, washed twice with a fixative (methanol/glacial acetic acid = 3:1, v/v), dropped onto slides, air-dried, and stained with a Giemsa stain. A total of 200 metaphase cells from each concentration were examined and scored for chromosome aberrations. Compound **3a-P1-HCl** was tested at 0.563, 1.125, 2.25, and 4.5 μg/mL for the chromosome analysis. A statistical analysis of the chromosome aberration data was performed using TOXSTAT2006 software.

Mice Bone Marrow Micronucleus Assay. An animal care and use application for the study was approved by the Institutional Animal Care and Use Committee of Shandong XinBo Pharmaceutical R&D Ltd. Compound **3a-P1-HCl** was subjected to the assay in ICR mice (male, $n = 60$) weighing 23.5 to 30.9 g. The mice were randomly divided into five groups (solvent control, positive control, and **3a-P1-HCl** at dose levels of 25, 50, and 100 mg/kg) with 12 mice in per group. Mice were dosed with the vehicle control and the tested article via oral gavage. At 24 and 48 h after dosing, animals were sacrificed for the bone marrow harvest. The bone marrow from each animal was examined microscopically to determine the micronucleus frequency and the proportion of polychromatic erythrocyte to total erythrocytes. A statistical analysis was performed using TOXSTAT2006 software.

Single-Dose Toxicity Studies. An animal care and use application for the study was approved by the Institutional Animal Care and Use Committee of Shandong XinBo Pharmaceutical R&D Ltd. ICR mice (40♀ and 40♂) were housed in standard SPF facilities. After at least 10 days of acclimation, mice were randomly divided into four groups (solvent control and the tested compound **3a-P1-HCl** at dose levels of 100, 200, and 300 mg/kg) with 20 mice in per group. Different doses of the tested compound were administered by oral gavage to the animals. Body weight, health, mortality, and clinical signs were monitored for a continuous period of 21 days during the study. After the recovery period, all animals were euthanized and dissected. Histopathological examinations of tissue samples were conducted.

Kinase Inhibitory Activity Assays. The kinases assayed were ABL1, ABL (E255K), ABL (F317I), ABL (G250E), ABL (H396P), ABL (M351T), ABL (Q252H), ABL (T315I), ABL (Y253F), c-Kit, c-Src, FGFR1, FLT3, KDR/VEGFR2, LYN, PDGFR, and TIE2/TEK. The substrate for ABL1 and its mutants and FLT3 was EAIYAAPFAKKK at 20 mM; the substrate for the kinases c-Kit, c-Src, KDR/VEGFR2, LYN, PDGFRa, and TIE2/TEK was poly-[Glu:Tyr](4:1) at 0.2 mg/mL; the substrate for FGFR1 was KKKSPGEYVNIIEFG at 20 mM. The reaction buffer was 20 mM HEPES (pH 7.5), 10 mM MgCl₂, 1 mM EGTA, 0.02% Brij35, 0.02 mg/mL BSA, 0.1 mM Na₃VO₄, 2 mM DTT, and 1% DMSO. The

kinase substrate was added into the reaction buffer, then the kinase was added. Compounds at the indicated concentrations were then delivered to the reaction using an echo liquid handler, and the mixture was incubated for 30 min at room temperature. Then, a ³³P-ATP solution (the concentration of ATP was 0.01 mCi/mL) was added to initiate the reaction, and the mixture was further incubated for 2 h at room temperature. The resulting reaction was filtered through an ion-exchange filter P81 (Whatman) and washed with 0.75% phosphoric acid three times to remove the ³³P-ATP without adding the substrate polypeptide. Finally, the ³³P-ATP samples on the filter paper were quantified with a liquid scintillator. The data shown are the mean value of three experiments.

■ ASSOCIATED CONTENT

Supporting Information

The Supporting Information is available free of charge at <https://pubs.acs.org/doi/10.1021/acs.jmedchem.1c00082>.

Synthesis of compounds **17a–e**, crystal data for compound **29**, SFC report for compounds **3a** and **3b**, and the determination of the absolute configuration of compound (**S**)-**23** (PDF)

Molecular formula strings (CSV)

X-ray crystal structure data for compound **29** (CIF)

■ AUTHOR INFORMATION

Corresponding Authors

Huanjie Shao – College of Life Sciences, Shaanxi Normal University, Xi'an 710119, P. R. China; Email: hshao@snnu.edu.cn

Chunrong Yu – Taizhou Astar BioTechnology Co. Ltd, Taizhou 225300, P. R. China; Email: yuc804@gmail.com

Haihong Huang – Beijing Key Laboratory of Active Substance Discovery and Druggability Evaluation, Institute of Materia Medica, Peking Union Medical College and Chinese Academy of Medical Sciences, Beijing 100050, P. R. China; Email: joyce@imm.ac.cn

Authors

Dongfeng Zhang – Beijing Key Laboratory of Active Substance Discovery and Druggability Evaluation, Institute of Materia Medica, Peking Union Medical College and Chinese Academy of Medical Sciences, Beijing 100050, P. R. China; orcid.org/0000-0003-0870-3782

Peng Li – Beijing Key Laboratory of Active Substance Discovery and Druggability Evaluation, Institute of Materia Medica, Peking Union Medical College and Chinese Academy of Medical Sciences, Beijing 100050, P. R. China

Yongxin Gao – Beijing Key Laboratory of Active Substance Discovery and Druggability Evaluation, Institute of Materia Medica, Peking Union Medical College and Chinese Academy of Medical Sciences, Beijing 100050, P. R. China

Yaoyao Song – College of Life Sciences, Shaanxi Normal University, Xi'an 710119, P. R. China

Yaquin Zhu – College of Life Sciences, Shaanxi Normal University, Xi'an 710119, P. R. China

Hong Su – College of Life Sciences, Shaanxi Normal University, Xi'an 710119, P. R. China

Beibei Yang – Beijing Key Laboratory of Active Substance Discovery and Druggability Evaluation, Institute of Materia Medica, Peking Union Medical College and Chinese Academy of Medical Sciences, Beijing 100050, P. R. China

Li Li – Beijing Key Laboratory of Active Substance Discovery and Druggability Evaluation, Institute of Materia Medica, Peking Union Medical College and Chinese Academy of

Medical Sciences, Beijing 100050, P. R. China; orcid.org/0000-0002-9496-2280

Gang Li – Beijing Key Laboratory of Active Substance Discovery and Druggability Evaluation, Institute of Materia Medica, Peking Union Medical College and Chinese Academy of Medical Sciences, Beijing 100050, P. R. China; orcid.org/0000-0003-0924-7950

Ningbo Gong – Beijing Key Laboratory of Polymorphic Drugs, Institute of Materia Medica, Peking Union Medical College and Chinese Academy of Medical Sciences, Beijing 100050, P. R. China

Yang Lu – Beijing Key Laboratory of Polymorphic Drugs, Institute of Materia Medica, Peking Union Medical College and Chinese Academy of Medical Sciences, Beijing 100050, P. R. China; orcid.org/0000-0002-2274-5703

Complete contact information is available at: <https://pubs.acs.org/10.1021/acs.jmedchem.1c00082>

Author Contributions

[†]These authors contributed equally.

Notes

The authors declare no competing financial interest.

ABBREVIATIONS USED

Ames, bacterial reverse mutation; BCR-ABL, breakpoint cluster region-abelson leukemia virus; CML, chronic myeloid leukemia; c-KIT, proto-oncogene that encodes a type III transmembrane tyrosine kinase; DMSO, dimethyl sulfoxide; DMF, *N,N*-dimethylformamide; DIPEA, diisopropyl ethylamine; DMAP, 4-dimethylaminopyridine; DEA, diethylamine; EDCl, 1-(3-(dimethylamino)-propyl)-3-ethylcarbodiimide hydrochloride; EtOAc, ethyl acetate; ECD, electronic circular dichroism; FGFR, fibroblast growth factor receptor; FLT3, FMS-like tyrosine kinase-3; HOBt, 1-hydroxybenzotriazole; hERG, human ether-a-go-go-related gene; LYN, Lck/Yes-related novel protein tyrosine kinase; PDGFR, platelet-derived growth factor receptor; PE, petroleum ether; PK, pharmacokinetic; Src, sarcoma; SAR, structure–activity relationship; SFC, supercritical fluid chromatography; TIE2/TEK, tyrosine kinase with immunoglobulin and EGF-like domains; TGI, tumor growth inhibition; TFA, trifluoroacetic acid; THF, tetrahydrofuran; VEGFR, vascular endothelial growth factor receptor

REFERENCES

- (1) Loscocco, F.; Visani, G.; Galimberti, S.; Curti, A.; Isidori, A. BCR-ABL independent mechanisms of resistance in chronic myeloid leukemia. *Front. Oncol.* **2019**, *9*, 939.
- (2) Jabbour, E.; Kantarjian, H. Chronic myeloid leukemia: 2020 update on diagnosis, therapy and monitoring. *Am. J. Hematol.* **2020**, *95*, 691–709.
- (3) Capdeville, R.; Buchdunger, E.; Zimmermann, J.; Matter, A. Glivec (STI571, imatinib), a rationally developed, targeted anticancer drug. *Nat. Rev. Drug Discovery* **2002**, *1*, 493–502.
- (4) Druker, B. J.; Guilhot, F.; O'Brien, S. G.; Gathmann, I.; Kantarjian, H.; Gattermann, N.; Deininger, M. W.; Silver, R. T.; Goldman, J. M.; Stone, R. M.; Cervantes, F.; Hochhaus, A.; Powell, B. L.; Gabrilove, J. L.; Rousselot, P.; Reiffers, J.; Cornelissen, J. J.; Hughes, T.; Agis, H.; Fischer, T.; Verhoef, G.; Shepherd, J.; Saglio, G.; Gratwohl, A.; Nielsen, J. L.; Radich, J. P.; Simonsson, B.; Taylor, K.; Baccarani, M.; So, C.; Letvak, L.; Larson, R. A. Five-year follow-up of patients receiving imatinib for chronic myeloid leukemia. *N. Engl. J. Med.* **2006**, *355*, 2408–2417.

(5) le Coutre, P.; Ottmann, O. G.; Giles, F.; Kim, D. W.; Cortes, J.; Gattermann, N.; Apperley, J. F.; Larson, R. A.; Abruzzese, E.; O'Brien, S. G.; Kuliczowski, K.; Hochhaus, A.; Mahon, F. X.; Saglio, G.; Gobbi, M.; Kwong, Y. L.; Baccarani, M.; Hughes, T.; Martinelli, G.; Radich, J. P.; Zheng, M.; Shou, Y.; Kantarjian, H. Nilotinib (formerly AMN107), a highly selective BCR-ABL tyrosine kinase inhibitor, is active in patients with imatinib-resistant or -intolerant accelerated-phase chronic myelogenous leukemia. *Blood* **2008**, *111*, 1834–1839.

(6) Shah, N. P.; Tran, C.; Lee, F. Y.; Chen, P.; Norris, D.; Sawyers, C. L. Overriding imatinib resistance with a novel ABL kinase inhibitor. *Science* **2004**, *305*, 399–401.

(7) Puttini, M.; Coluccia, A. M.; Boschelli, F.; Cleris, L.; Marchesi, E.; Donella-Deana, A.; Ahmed, S.; Redaelli, S.; Piazza, R.; Magistrini, V.; Andreoni, F.; Scapozza, L.; Formelli, F.; Gambacorti-Passerini, C. In vitro and in vivo activity of SKI-606, a novel Src-Abl inhibitor, against imatinib-resistant Bcr-Abl+ neoplastic cells. *Cancer Res.* **2006**, *66*, 11314–11322.

(8) Roychowdhury, S.; Talpaz, M. Managing resistance in chronic myeloid leukemia. *Blood Rev.* **2011**, *25*, 279–290.

(9) Huang, W. S.; Metcalf, C. A.; Sundaramoorthi, R.; Wang, Y.; Zou, D.; Thomas, R. M.; Zhu, X.; Cai, L.; Wen, D.; Liu, S.; Romero, J.; Qi, J.; Chen, I.; Banda, G.; Lentini, S. P.; Das, S.; Xu, Q.; Keats, J.; Wang, F.; Wardwell, S.; Ning, Y.; Snodgrass, J. T.; Broudy, M. I.; Russian, K.; Zhou, T.; Commodore, L.; Narasimhan, N. I.; Mohemmad, Q. K.; Iulucci, J.; Rivera, V. M.; Dalgarno, D. C.; Sawyer, T. K.; Clackson, T.; Shakespeare, W. C. Discovery of 3-[2-(imidazo[1,2-b]pyridazin-3-yl)ethynyl]-4-methyl-*N*-{4-[(4-methylpiperazin-1-yl)methyl]-3-(trifluoromethyl)phenyl}benzamide (AP24534), a potent, orally active pan-inhibitor of breakpoint cluster region-abelson (BCR-ABL) kinase including the T315I gatekeeper mutant. *J. Med. Chem.* **2010**, *53*, 4701–4719.

(10) O'Hare, T.; Shakespeare, W. C.; Zhu, X.; Eide, C. A.; Rivera, V. M.; Wang, F.; Adrian, L. T.; Zhou, T.; Huang, W. S.; Xu, Q.; Metcalf, C. A.; 3rd; Tyner, J. W.; Loriaux, M. M.; Corbin, A. S.; Wardwell, S.; Ning, Y.; Keats, J. A.; Wang, Y.; Sundaramoorthi, R.; Thomas, M.; Zhou, D.; Snodgrass, J.; Commodore, L.; Sawyer, T. K.; Dalgarno, D. C.; Deininger, M. W.; Druker, B. J.; Clackson, T. AP24534, a pan-BCR-ABL inhibitor for chronic myeloid leukemia, potently inhibits the T315I mutant and overcomes mutation-based resistance. *Cancer Cell* **2009**, *16*, 401–412.

(11) Nicolini, F. E.; Basak, G. W.; Kim, D. W.; Olavarria, E.; Pinilla-Ibarz, J.; Apperley, J. F.; Hughes, T.; Niederwieser, D.; Mauro, M. J.; Chuah, C.; Hochhaus, A.; Martinelli, G.; DerSarkissian, M.; Duh, M. S.; McGarry, L. J.; Kantarjian, H. M.; Cortes, J. E. Overall survival with ponatinib versus allogeneic stem cell transplantation in Philadelphia chromosome-positive leukemias with the T315I mutation. *Cancer* **2017**, *123*, 2875–2880.

(12) Nicolini, F. E.; Mauro, M. J.; Martinelli, G.; Kim, D. W.; Soverini, S.; Muller, M. C.; Hochhaus, A.; Cortes, J.; Chuah, C.; Dufva, I. H.; Apperley, J. F.; Yagasaki, F.; Pearson, J. D.; Peter, S.; Sanz Rodriguez, C.; Preudhomme, C.; Giles, F.; Goldman, J. M.; Zhou, W. Epidemiologic study on survival of chronic myeloid leukemia and Ph⁺ acute lymphoblastic leukemia patients with BCR-ABL T315I mutation. *Blood* **2009**, *114*, 5271–5278.

(13) Ivanova, E. S.; Tatarskiy, V. V.; Yastrebova, M. A.; Khamidullina, A. I.; Shunaev, A. V.; Kalina, A. A.; Zeifman, A. A.; Novikov, F. N.; Dutikova, Y. V.; Chilov, G. G.; Shtil, A. A. PF114, a novel selective inhibitor of BCR-ABL tyrosine kinase, is a potent inducer of apoptosis in chronic myelogenous leukemia cells. *Int. J. Oncol.* **2019**, *55*, 289–297.

(14) Tanaka, R.; Squires, M. S.; Kimura, S.; Yokota, A.; Nagao, R.; Yamauchi, T.; Takeuchi, M.; Yao, H.; Reule, M.; Smyth, T.; Lyons, J. F.; Thompson, N. T.; Ashihara, E.; Ottmann, O. G.; Maekawa, T. Activity of the multitargeted kinase inhibitor, AT9283, in imatinib-resistant BCR-ABL-positive leukemic cells. *Blood* **2010**, *116*, 2089–2095.

(15) Howard, S.; Berdini, V.; Boulstridge, J. A.; Carr, M. G.; Cross, D. M.; Curry, J.; Devine, L. A.; Early, T. R.; Fazal, L.; Gill, A. L.; Heathcote, M.; Maman, S.; Matthews, J. E.; McMenamin, R. L.;

Navarro, E. F.; O'Brien, M. A.; O'Reilly, M.; Rees, D. C.; Reule, M.; Tisi, D.; Williams, G.; Vinkovic, M.; Wyatt, P. G. Fragment-based discovery of the pyrazol-4-yl urea (AT9283), a multitargeted kinase inhibitor with potent aurora kinase activity. *J. Med. Chem.* **2009**, *52*, 379–388.

(16) Ren, X.; Pan, X.; Zhang, Z.; Wang, D.; Lu, X.; Li, Y.; Wen, D.; Long, H.; Luo, J.; Feng, Y.; Zhuang, X.; Zhang, F.; Liu, J.; Leng, F.; Lang, X.; Bai, Y.; She, M.; Tu, Z.; Pan, J.; Ding, K. Identification of GZD824 as an orally bioavailable inhibitor that targets phosphorylated and nonphosphorylated breakpoint cluster region-Abelson (Bcr-Abl) kinase and overcomes clinically acquired mutation-induced resistance against imatinib. *J. Med. Chem.* **2013**, *56*, 879–894.

(17) Zhang, D.; Li, P.; Lin, Z.; Huang, H. An efficient and convenient protocol for the synthesis of 1,1-difluoro-6-nitro-2,3-dihydro-1H-indene derivatives. *Synthesis* **2014**, *46*, 613–620.